

International Journal of Modern Physics A
 ©World Scientific Publishing Company

BLACK HOLES IN THEORIES WITH LARGE EXTRA DIMENSIONS: A REVIEW

PANAGIOTA KANTI

*Theoretical Physics, University of Oxford, 1 Keble Road,
 Oxford OX1 3NP, United Kingdom*

We start by reviewing the existing literature on the creation of black holes during high-energy particle collisions, both in the absence and in the presence of extra, compact, spacelike dimensions. Then, we discuss in detail the properties of the produced higher-dimensional black holes, namely the horizon radius, temperature and life-time, as well as the physics that governs the evaporation of these objects, through the emission of Hawking radiation. We first study the emission of *visible* Hawking radiation on the brane: we derive a *master* equation for the propagation of fields with arbitrary spin in the induced-on-the-brane black hole background, and we review all existing results in the literature for the emission of scalars, fermions and gauge bosons during the *spin-down* and *Schwarzschild* phases of the life of the black hole. Both analytical and numerical results for the greybody factors and radiation spectra are reviewed and exact results for the number and type of fields emitted on the brane as a function of the dimensionality of spacetime are discussed. We finally study the emission of Hawking radiation in the bulk: greybody factors and radiation spectra are presented for the emission of scalar modes, and the ratio of the *missing* energy over the *visible* one is calculated for different values of the number of extra dimensions.

Keywords: Black Holes; Large Extra Dimensions; Hawking Radiation.

1. Introduction

A few years ago, in 1998, a novel idea was proposed according to which the so-called *hierarchy problem* – in other words, our difficulty in answering the question of why the characteristic scale of gravity, $M_P \sim 10^{19}$ GeV, is 16 orders of magnitude larger than the Electro-Weak scale, $M_{EW} \sim 1$ TeV – could be solved by assuming the existence of extra dimensions in the Universe^{1,2}. The novelty in this idea was that the traditional picture of Planck-length-sized additional spacelike dimensions ($\ell_P \simeq 10^{-33}$ cm) was abandoned, and the extra dimensions could have a size as large as 1 mm. The upper bound on the size of the proposed *Large Extra Dimensions* actually matched the smallest length scale down to which the force of the gravitational interactions, and thus their $1/r^2$ dependence, had been measured. If extra dimensions of that size did exist, gravitational interactions would have a completely different dependence on r in scales smaller than 1 mm, however no gravitational experiment at that time could rule this out.

On the other hand, electromagnetic, weak and strong forces are indeed sensitive to the existence of extra dimensions. If, for example, gauge bosons were allowed to propagate in the extra-dimensional spacetime, their interactions would be modified beyond any acceptable phenomenological limits unless the size of the extra dimensions was smaller than 10^{-16} cm. This problem was resolved under the assumption that all particles experiencing this type of interactions, in other words, all ordinary matter, is restricted to live on a (3+1)-dimensional hypersurface, a *3-brane*, that has a width along the extra dimensions of, at most, the above order. The 3-brane, playing the role of our four-dimensional world, is then embedded in the higher-dimensional spacetime, usually called the *bulk*, in which only gravity can propagate.

In this model, the large volume of the extra dimensions can help us solve, or at least recast, the hierarchy problem: the traditional Planck scale, M_{Pl} , is only an effective energy scale derived from the fundamental higher-dimensional one, M_* , through the following relation ¹

$$M_P^2 \sim M_*^{2+n} R^n. \quad (1)$$

In the above, it has been assumed that each one of the extra spacelike, compact dimensions has the same size R . From the above, it becomes clear that, if the volume of the compact space, $V \sim R^n$, is large, i.e if $R \gg \ell_P$, then the $(4+n)$ -dimensional Planck mass, M_* , will be much lower than the 4-dimensional one, M_P . If one chooses $M_* = M_{EW}$, then the above expression provides a relation between the scale of gravity and the scale of particle interactions.

The above idea makes use of geometrical features of the extra, compact space in order to connect two completely different energy scales. The same goal was achieved by an alternative, but similar idea, that was proposed a year later ³ (for some early works on brane-world models and their implications, see Refs. 4-9). According to this alternative proposal, the magnitude of the effective energy scale on the 3-brane, taken to be of the order of the Electro-Weak scale, follows from the fundamental higher-dimensional scale M_P after being suppressed by an exponential factor involving the distance of our observable brane from a hidden brane. In both models, however, the complete resolution of the hierarchy problem would demand also an explanation of why the volume of the compact space, or the inter-brane distance, has the value that leads to the observed ratio of M_P/M_{EW} .

In this review, we will concentrate on the scenario with Large Extra Dimensions. A number of experiments and theoretical analyses have tried over the years to put bounds on the size of extra, compact dimensions, and the produced bounds are constantly updated. In the regime $r \ll R$, the extra dimensions ‘open up’ and Newton’s law for the gravitational interactions is modified assuming a $1/r^{n+2}$ dependence on the radial separation between two massive particles. Torsion-balance experiments which measure the gravitational inverse-square law at short scales can provide limits on the size of the extra dimensions, or equivalently on the value of the fundamental scale M_* . On the other hand, since gravitons can propagate both in

Table 1. Current limits on the size of extra, compact dimensions

Type of Experiment/Analysis	$M_* \geq$	$M_* \geq$
Collider limits on the production of real or virtual KK gravitons ^{10,11,12}	1.45 TeV ($n = 2$)	0.6 TeV ($n = 6$)
Torsion-balance Experiments ¹³	3.5 TeV ($n = 2$)	
Overclosure of the Universe ¹⁴	8 TeV ($n = 2$)	
Supernovae cooling rate ^{15,16,17,18}	30 TeV ($n = 2$)	2.5 TeV ($n = 3$)
Non-thermal production of KK modes ¹⁹	35 TeV ($n = 2$)	3 TeV ($n = 6$)
Diffuse gamma-ray background ^{14,20,21}	110 TeV ($n = 2$)	5 TeV ($n = 3$)
Thermal production of KK modes ²¹	167 TeV ($n = 2$)	1.5 TeV ($n = 5$)
Neutron star core halo ²²	500 TeV ($n = 2$)	30 TeV ($n = 3$)
Neutron star surface temperature ²²	1700 TeV ($n = 2$)	60 TeV ($n = 3$)
BH absence in neutrino cosmic rays ²³		1-1.4 TeV ($n \geq 5$)

the bulk and on the brane, massive Kaluza-Klein (KK) graviton states can modify both the cross sections of Standard Model particle interactions and astrophysical or cosmological processes. Assuming modifications that are below the current observable limits puts bounds on the mass of the KK gravitons, and consequently, on the size of extra dimensions. In Table 1, we summarize some of those limits. The constraints from collider experiments, although more accurate, are particularly mild, while the cosmological and astrophysical ones are much more stringent; however, they contain large systematic errors. If we ignore these errors, the latter type of constraints exclude by far even the $n = 3$ case, while low-gravity models with $M_* \sim 1$ TeV are still allowed for $n \geq 4$.

If indeed present, the extra dimensions will inevitably change our notion for the universe. The introduction of extra dimensions affects both gravitational interactions and particle physics phenomenology, and leads to modifications in standard cosmology. Already existing theories would need to be extended or modified in order to accommodate the effects resulting from the presence of extra dimensions (for an incomplete list of works on the cosmological and phenomenological implications in theories with large extra dimensions, see Refs. 24-47). Similarly, the properties and physics of black holes are also bound to change in the context of a higher-dimensional theory.

As in the four-dimensional case, it seems natural to assume that, when matter trapped on the brane undergoes gravitational collapse, a black hole is formed which is centered on the brane and extends along the extra dimensions. If the horizon of the formed black hole is much larger than the size of the extra dimensions, $r_H \gg R$, the produced black hole is effectively a four-dimensional object. If, however, $r_H \ll R$, then this small black hole is virtually a higher-dimensional object that is completely submerged into the extra-dimensional spacetime. As we will see, these small black

holes have significantly modified properties compared to a four-dimensional black hole with exactly the same mass M_{BH} : for example, they are larger, colder and thus live longer compared to their four-dimensional analogues. Another striking consequence of the introduction of extra dimensions is that, by lowering the Planck scale M_* closer to the Electro-Weak scale, the idea of the production of miniature black holes during high-energy scattering processes, with trans-Planckian center-of-mass energy $\sqrt{s} \gg M_*$, now becomes more realistic. Theoretical arguments have shown that the presence of the extra dimensions facilitates further the production of black holes during such collisions by increasing the production cross-section, thus leading to striking consequences for the high-energy interactions of elementary particles either at colliders or at cosmic rays.

The produced black holes are characterized by a non-vanishing temperature T_H , whose value is inversely proportional to the horizon radius. They decay by the emission of Hawking radiation, i.e. emission of elementary particles with rest mass smaller than T_H . This is expected to be their most prominent observable signature with a characteristic thermal radiation spectrum and an almost blackbody profile. The non-trivial metric in the region exterior to the horizon of the black hole creates an effective potential barrier which backscatters a part of the outgoing radiation back into the black hole. The amount of radiation that finally reaches the observer at infinity depends on the *energy* of the emitted particle, its *spin* and the *dimensionality* of spacetime. The dependence on all the aforementioned parameters is encoded into the expression of a filtering function, the ‘greybody factor’ $\sigma_n^{(s)}(\omega)$, which is present in the radiation spectrum. The greybody factors can be important experimentally since they modify the spectrum in the low- and intermediate-energy regime, where most particles are produced, thus altering the characteristic spectrum by which we hope to identify a ‘BH event’. In addition, as we will explain later in this review, by studying the Hawking radiation emitted by this type of small black holes, one would be able to ‘read’ the total number of dimensions that exist in nature.

A higher-dimensional black hole emits radiation both in the bulk and on the brane. According to the assumptions of the theory with Large Extra Dimensions, only gravitons, and possibly scalar fields, can propagate in the bulk and thus, these are the only types of fields allowed to be emitted in the bulk during the Hawking evaporation phase. On the other hand, the emission on the brane can take the form of scalar Higgs particles, fermions and gauge bosons. From the perspective of the brane observer, the radiation emitted in the bulk will be a missing energy signal, while radiation on the brane may lead to experimental detection of Hawking radiation and thus of the production of small black holes. Nevertheless, in order to have a clear picture of the characteristics of the radiation spectrum on the brane, it is important to know exactly how much energy is lost in the bulk.

As we mentioned above, the greybody factor depends on the dimensionality of spacetime; it also depends on whether the emitted particle is brane-localized or free to propagate in the bulk. The greybody factor is actually the outgoing transmission cross-section associated with propagation in the aforementioned gravitational

background, however, due to the thermal character of the radiation spectrum, it is equal to the incoming absorption cross-section⁴⁸. Therefore, all we need to do is to solve the equation of motion of a particle incident on the background metric that describes the black hole, either higher-dimensional or four-dimensional. After the absorption coefficient is computed, the corresponding cross-section, and thus the greybody factor, can easily follow.

We need to stress here that the above semiclassical calculation of Hawking emission is only reliable when the energy of the emitted particle is small compared to the black hole mass, $\omega \ll M_{BH}$, since only in this case is it correct to neglect the back reaction of the metric during the emission process. This in turn requires that the Hawking temperature obeys the relation $T_H \ll M_{BH}$, which is equivalent to demanding that the black hole mass $M_{BH} \gg M_*$. As the decay proceeds and the mass of the black hole decreases, inevitably this condition will break down during the final stages of the evaporation process. Nevertheless, for black holes of initial mass much larger than M_* most of the evaporation process is within the semi-classical regime.

We will start this article by reviewing, in Section 2, the existing literature on the creation of black holes during high-energy particle collisions, both in four-dimensional and higher-dimensional spacetimes. In Section 3, we will discuss the properties of the produced higher-dimensional black holes, namely the horizon radius, the temperature and their life-time, and point out the differences between them and their four-dimensional analogues. The physics that governs the evaporation of these higher-dimensional objects, through the emission of Hawking radiation, is covered in Section 4. Section 5 focuses on the emission of Hawking radiation directly on the brane: we start with the derivation of the *master* equation for the propagation of fields with arbitrary spin in the induced-on-the-brane black hole background, and then we present all existing results in the literature for the emission of scalars, fermions and gauge bosons during the *spin-down* and *Schwarzschild* phases of the life of the black hole; both analytical and numerical results for the greybody factors and radiation spectra are presented as well as exact results for the number and type of fields emitted on the brane as a function of the dimensionality of space-time. Section 6 deals with the emission of Hawking radiation in the bulk and the question of the amount of the missing energy: analytical and numerical results on the emission of bulk scalar fields, including greybody factors and radiation spectra, are reviewed, and the ratio of the missing energy over the ‘visible’ one emitted on the brane is presented for the Schwarzschild phase and for different values of the number of extra dimensions. Our conclusions are summarized in Section 7.

2. High-energy Collisions and Black Hole Creation

If extra dimensions do exist and the fundamental scale of gravity is much lower than the traditional Planck scale M_P , then in the near future we will witness collisions of particles with trans-Planckian energies, i.e. energies larger than the fun-

damental Planck scale M_* . Although, as we approach M_* , quantum gravity effects become important for elementary particles, another semi-classical regime opens up for center-of-mass energies of the colliding particles $\sqrt{s} \gg M_*$: the products of such a collision would have a mass much larger than the scale of quantum gravity and for these objects (as for any macroscopic object) quantum gravity effects can be safely ignored.

The high-energy scattering of particles and the nature of the products of such collisions have been investigated in the framework of the General Theory of Relativity^{49,50,51,52,53}, String Theory^{54,55} and Quantum Gravity^{56,57}. The usual approach followed is that the relativistic colliding particles (or black holes) may be described by two Aichelburg-Sexl gravitational shock waves. In the limit of moving velocity equal to the speed of light, the two particles can be considered massless and the curvature is zero except on the null plane of their trajectory. If the impact parameter b is larger than the Schwarzschild radius r_H , that corresponds to the center-of-mass energy of the two particles, elastic and inelastic processes will in general take place between the two shock-waves accompanied by the exchange of gravitons. If on the other hand, $b \leq r_H$, then, according to the General Theory of Relativity and the “hoop-conjecture”⁵⁸, strong gravitational effects will dominate and a black hole will be formed. The production cross-section, in this high-energy limit, is given by the geometrical cross-section

$$\sigma \sim \pi b^2 \sim \pi r_H^2, \quad (2)$$

i.e. by the “target” area defined by the impact parameter.

As reported in Ref. 53, Penrose found a lower bound on the mass of the black hole produced during the collision of two particles moving at the speed of light⁵⁹. On the union of the two null planes, that describe the trajectories of the two particles, an apparent horizon is formed, with an area of $32\pi\mu^2$ where μ is the energy of each particle in the center-of-mass coordinate frame. This sets a lower bound on the area of the event horizon (that according to the Cosmic Censorship hypothesis⁶⁰ lies outside the apparent horizon) and thus on the mass of the produced black hole; this is found to be

$$M_{BH} \geq \frac{1}{\sqrt{2}} 2\mu, \quad (3)$$

leading to the conclusion that at least 71% of the initial center-of-mass energy of the colliding particles will be bound into the black hole. The perturbative analysis done subsequently in Ref. 53 determined the amount of energy spent into gravitational radiation during the collision to be 16% of the total energy, thus raising the estimate of the mass of the black hole to 84% of \sqrt{s} . The above results were derived under the assumption of head-on collision ($b = 0$) in four-dimensional spacetime. An alternative study of the high-energy collision of a particle with a Schwarzschild black hole in four dimensions⁶¹ led to a similar result: the emission of gravitational radiation is approximately 13% of the initial energy of the system; in the case of

a rotating black hole, however, this percentage can become as large as 35%, but decreases as the impact parameter increases.

After the theories with large extra dimensions and a low-scale gravity were proposed¹, the idea of the creation of black holes from the collision of particles with trans-Planckian energies was revived⁶². The need for the update of the above lower limit on the mass of the black hole for an arbitrary number of spacelike dimensions was obvious. Moreover, realistic calculations of the rate of production of black holes during particle collisions demanded the generalization of the same analysis for non-zero impact parameters. By investigating the formation of a closed-trapped surface around the colliding particles/shock-waves, the authors of Ref. 63 have shown that such surfaces do indeed form for both $D = 4$ and $D > 4$ upon particular assumptions for the value of the impact parameter. Of particular importance was their result that, in $D = 4$, black holes form if, and only if, $b < b_{max} \simeq 0.8r_H$, a result which reduces the value of the cross-section to $\sigma \simeq 0.65\pi r_H^2$, and sets the range of the black hole mass to

$$M_{BH} = (0.71 - 0.45)\sqrt{s}, \quad \text{for } b = \{0, b_{max}\}. \quad (4)$$

Their higher-dimensional analysis, performed only for head-on collisions ($b = 0$), revealed that the lower bound on the mass of the produced black hole decreases also with the number of extra dimensions reaching $0.58\sqrt{s}$ for $D = 11$. In Ref. 64, it was found that, for head-on collisions and as D increases, the circumference of the region into which the mass M must be compacted to produce a black hole is a decreasing fraction of $2\pi r_H$. The same authors also showed that, for $b \neq 0$, the value of b_{max} that can produce a black hole increases with D and is given by:

$$b_{max} \sim 2^{-1/(D-3)}r_H. \quad (5)$$

This leads to the enhancement of the production cross-section, nevertheless, the mass of the produced black hole will still be suppressed for large values of D , in agreement with the results of Ref. 63. A recent numerical analysis⁶⁵ has produced some new estimates for the energy lost in the form of gravitational radiation during a head-on collision in a higher-dimensional spacetime: 13% for $D = 4$ to 8% for $D = 10$. While the former result is in agreement with Refs. 53 and 61, the latter seems to disagree with the results produced by the authors of Refs. 63 and 64. The apparent disagreement can be resolved only under the assumption that a significant part of the energy lost in the collision has a form different from that of gravitational radiation.

The formation of closed-trapped surfaces was studied analytically in Ref. 66 for the more realistic case of finite-front shock-waves, and was shown to indeed take place for $D \geq 4$ and for an arbitrary impact parameter. The effect of the angular momentum was looked at in Ref. 67, where it was argued that the production cross-section gets further enhanced when the spinning of the black hole is taken into account. Finally, the evolution of the closed-trapped surfaces in time was studied in Ref. 68.

But where and when these black holes may be produced? In the context of theories with large extra dimensions, the trans-Planckian energy regime may lie slightly above the TeV scale. This raises the exciting possibility that particle collisions with trans-Planckian energies may take place, in the near future, at ground-based accelerators^{69,70,71,72,73}, or they may even already take place in the atmosphere of the earth^{74,75,76,77}. In the first case, accelerated particles (protons or nuclei) collide at center-of-mass energies $\sqrt{s} > M_*$ at ground-based accelerators; if the impact parameter is smaller than a critical value b_c , a higher-dimensional black hole will be formed. The same holds in the case where highly-energetic cosmic ray particles with energies up to 100 TeV collide with particles in the atmosphere of the earth. Neutrinos being scattered by nuclei are expected to be the most effective source of black hole production from cosmic ray particles due to the absence of any QCD-type contaminating effects and small Standard-Model cross-sections.

The corresponding black hole production cross-sections are calculated in both cases in the same way: first, any pair of partons (i, j) that pass within the Schwarzschild radius, i.e. have $b < b_c \simeq r_H(s)$, can lead to the production of a black hole with cross-section $\sigma_{ij} \simeq \pi r_H^2(s)$, where \sqrt{s} is the center-of-mass energy of the colliding particles. However, in a realistic collision, the colliding particles consist of more than one partons, therefore, a summation must be made over all parton pairs that carry enough energy to produce a black hole of a minimum mass M_{min} . For this reason, the fraction of the center-of-mass energy that each parton carries must be taken into account via the use of the parton distribution functions $f_i(x)$, that give the probability of finding a parton with a fraction x of the momentum of the colliding particle. The total cross-section for the production of a black hole from the collision of two particles A and B may then be written as^{69,70}

$$\sigma_{AB \rightarrow bh}(\tau_m, s) = \sum_{i,j} \int_{\tau_m}^1 d\tau \int_{\tau}^1 \frac{dx}{x} f_i(x) f_j\left(\frac{\tau}{x}\right) \sigma_{ij}(\tau s), \quad (6)$$

where $\tau = x_i x_j$ is the parton-parton center-of-mass energy squared fraction, and $\sqrt{\tau_m s}$ is the minimum center-of-mass energy necessary for the creation of the minimum black hole mass, $M_{min} \simeq \sqrt{\tau_m s}$. In the above, it has been assumed that both colliding particles are composite – in case one of the particles is elementary (i.e. neutrinos) this expression is simplified⁷⁵. Early estimates found particularly large production cross-sections of black holes: high-energy neutrinos scattered by nuclei at the earth's atmosphere give a production cross-section, for a black hole with $M_{min} = M_* = 1$ TeV, which is two orders of magnitude larger than the cross-section of any similar Standard Model process⁷⁵. On the other hand, proton-proton scattering at the LHC with $M_* = 1$ TeV was found to lead to a production cross-section of 10^5 fb for $M_{min} = 5$ TeV, a large cross-section by new physics standards; for $M_{min} = 10$ TeV, the cross-section reduces to 10 fb. These estimates gave a substantial boost towards the further study of the production and phenomenology of black holes in theories with extra dimensions (see Refs. 78-105).

We should note here that the above production cross-sections decrease if one

takes into account the results of the studies on the formation of closed-trapped surfaces mentioned earlier in this section. By taking $b_c = r_H$ and not $b = b_{max}$, where b_{max} is only a fraction of the Schwarzschild horizon, we obviously obtain an overestimate of the production cross-section. Moreover, assuming that the available energy for the production of black hole is the whole of the center-of-mass energy \sqrt{s} is again an over-simplification since part of that energy is bound to be lost in the form of gravitational radiation during the collision⁵³. A claim for an additional suppression of this process was made¹⁰⁶ according to which an exponential suppression factor involving the Euclidean action of the system should be included. However further studies^{71,66,107} argued that the black hole creation process from the collision of two particles was not classically forbidden and this suppression factor should not be taken into account. Subsequent analyses^{108,109} calculated quantum corrections to the semi-classical cross-section and showed that these are indeed small. From a different perspective, the authors of Ref. 110 have claimed that the use of the generalized uncertainty principle leads to a radical increase in the minimum amount of energy that is necessary for the creation of a black hole, thus rendering unlikely the production of black holes at next-generation colliders such as the Large Hadron Collider (LHC) with a center-of-mass energy of 14 TeV. Recently, the validity of the description of the creation of a black hole from the collision of a pair of Aichelburg-Sexl shock-waves was also questioned¹¹¹, and the argument that strong-curvature and quantum gravity effects significantly alter the geometric cross-section estimate was put forward.

3. Properties of the Higher-Dimensional Mini Black Holes

As we will see below, in the absence of extra dimensions, the creation of a semi-classical black hole demands extremely large center-of-mass energies, which are far beyond our technical abilities. Reducing the mass of the black hole down to accessible energy scales simply leads to an unnaturally small Schwarzschild radius, which can never be attained. On the other hand, the presence of the extra dimensions facilitate the creation of black holes since it lowers the scale of quantum gravity, thus allowing the production of semi-classical black holes at lower energies, and increases the corresponding Schwarzschild radius for a given center-of-mass energy, thus making the black hole creation regime, $b \leq r_H$, more easily accessible.

Of particular importance, and simplicity, are the higher-dimensional black holes that have a horizon radius much smaller than the size of the extra dimensions, $r_H \ll R$. In this case, these mini black holes are completely submerged into a D -dimensional spacetime that, to a very good approximation, has one timelike and $D - 1$ non-compact spacelike coordinates. If we further assume that the produced black hole is spherically-symmetric, i.e. non-rotating, the gravitational background around this black hole is given by a generalized Schwarzschild line-element of the

form ¹¹²

$$ds^2 = \left[1 - \left(\frac{r_H}{r} \right)^{n+1} \right] dt^2 - \left[1 - \left(\frac{r_H}{r} \right)^{n+1} \right]^{-1} dr^2 - r^2 d\Omega_{2+n}^2, \quad (7)$$

where n stands for the number of extra, spacelike dimensions that exist in nature ($D = 4 + n$), and $d\Omega_{2+n}^2$ is the area of the $(2 + n)$ -dimensional unit sphere given by

$$d\Omega_{2+n}^2 = d\theta_{n+1}^2 + \sin^2 \theta_{n+1} \left(d\theta_n^2 + \sin^2 \theta_n \left(\dots + \sin^2 \theta_2 (d\theta_1^2 + \sin^2 \theta_1 d\varphi^2) \dots \right) \right). \quad (8)$$

In the above, $0 < \varphi < 2\pi$ and $0 < \theta_i < \pi$, for $i = 1, \dots, n + 1$. The line-element (7) can be easily shown to satisfy the vacuum $(4 + n)$ -dimensional Einstein's equations. The black hole is assumed to be bound on a 3-brane, our four-dimensional world, nevertheless, the tension of the brane is assumed to be much smaller than the black hole mass and thus it can be ignored in our analysis.

By using an analogous approach to the usual 4-dimensional Schwarzschild calculation, i.e. by applying Gauss' law in the $(4 + n)$ -dimensional spacetime, we obtain the following relation between the horizon radius and the mass M_{BH} of the black hole ¹¹²

$$r_H = \frac{1}{\sqrt{\pi} M_*} \left(\frac{M_{BH}}{M_*} \right)^{\frac{1}{n+1}} \left(\frac{8\Gamma(\frac{n+3}{2})}{n+2} \right)^{\frac{1}{n+1}}. \quad (9)$$

We notice that, for $n \neq 0$, the relation between r_H and M_{BH} is not linear anymore, and that it is the fundamental Planck scale M_* that appears in the expression of the horizon radius and not the four-dimensional one M_P . The latter feature is the main reason for the fact that extra dimensions facilitate the creation of low-mass black holes, as we will shortly see.

Before elaborating on this last point, we need to make another comment first: in order to be able to ignore quantum corrections in our calculations and study the produced black holes by using semi-classical methods, the mass of the black hole must be, at least, a few times larger than the scale of quantum gravity M_* . Therefore, if we assume that $M_* = 1$ TeV, a safe limit for the mass of the produced black hole would be ^{69,72} $M_{BH} = 5$ TeV. By keeping fixed the mass of the produced black hole, we may calculate the value of the horizon radius as a function of n ; these values are given in Table 2.

Table 2. Black hole horizon radii for different values of n

n	1	2	3	4	5	6	7
$r_H (10^{-4} \text{ fm})$	4.06	2.63	2.22	2.07	2.00	1.99	1.99

One may easily conclude, from the above, that during the collision of two particles, with a center-of-mass energy $\sqrt{s} \geq 5$ TeV, a black hole may be formed if the particles pass within an area of radius 10^{-4} fm; this is merely a sub-nuclear

distance attainable at particle physics experiments. On the other hand, in the absence of extra dimensions, the lightest semi-classical black hole would have a mass of, at least, a few times the four-dimensional Planck mass, $M_P \simeq 10^{16}$ TeV; the creation of a black hole from a high-energy collision would then demand center-of-mass energies higher than M_P , a requirement which is far beyond the reach of any present and future accelerator. Overlooking for the moment the fact that a four-dimensional black hole with $M_{BH} < M_P$ would not be a classical object, we may ask what would be the value of the Schwarzschild radius for an object with mass $M = 5$ TeV being produced in four dimensions in a high-energy collision. We find that the Schwarzschild radius for such an object has the extraordinary value of $r_H = 1.3 \times 10^{-50}$ m, i.e. 35 orders of magnitude smaller than the radius of the proton.

The modified properties of a higher-dimensional, Schwarzschild-like black hole, compared to those of a four-dimensional one with the same mass, were first studied in Ref. 113. The fact that the Schwarzschild radius in $D > 4$ dimensions is larger than the one in $D = 4$, for a given mass M_{BH} , was first pointed out in there, and further implications of the existence of extra dimensions on the temperature, lifetime and entropy of the black hole were investigated. We will now stop and look in some detail at the temperature of a higher-dimensional black hole to see where the difference from the four-dimensional case lies. The temperature of a $(4 + n)$ -dimensional black hole is given by the expression¹¹²

$$T_H = \frac{(n+1)}{4\pi r_H}. \quad (10)$$

Let us assume again that $M_* = 1$ TeV, and that the produced black hole has a mass $M_{BH} = 5$ TeV. By using Eq. (10) and the entries of Table 1, we may easily calculate the temperature of the produced black hole for different values of n ; the results are displayed in Table 3.

Table 3. Black hole temperatures for different values of n

n	1	2	3	4	5	6	7
T_H (GeV)	77	179	282	379	470	553	629

As we will shortly see, a black hole with a temperature T_H emits thermal radiation, the so-called Hawking radiation¹¹⁴, through the emission of ordinary particles. This leads to the decay of the black hole and finally to its evaporation. The radiation spectrum has a blackbody profile with the peak of the curve being at energies very close to its temperature. The temperature values displayed in Table 3 all lie in the GeV regime, which is the energy range that present and next-generation experiments can probe. We may, thus, conclude that the presence of extra dimensions, not only facilitates the creation of a black hole at a high-energy collision, but also renders more likely the detection of their most prominent feature, the emitted

Hawking radiation.

We should note here that Hawking radiation emitted by larger, and thus effectively four-dimensional, astrophysical black holes has never been observed. Taking $M_{BH} \simeq 3M_{\odot}$, which is the current upper limit on the mass of neutron stars, and using Eq. (10) with $n = 0$, we find that $T_H \simeq 10^{-12}$ eV = 20 nK; this is a very low temperature corresponding to a very low energy frequency, or a very large wavelength, that unfortunately cannot be detected. In the absence of extra dimensions, the only black holes that could emit radiation today at detectable frequencies, are primordial ones that were created at the early universe and can have a much lower mass. For example, a black hole with a mass $M_{BH} = 10^{15}$ gr should give a Hawking radiation spectrum with a peak in the area of 10-100 MeV; still, such a radiation has not been yet observed.

Combining Eqs. (9) and (10), we may conclude that, since a $(4+n)$ -dimensional small black hole has a horizon radius much larger than a four-dimensional one with the same mass, it will have a temperature in $D > 4$ which is much lower than the one in $D = 4$ ¹¹³. Indeed, if a ‘quantum’ black hole with $M_{BH} = 5$ TeV had been allowed to exist in nature in $D = 4$, its temperature would have been 30 orders of magnitude larger than the entries in Table 3. The larger the temperature of the black hole is, the faster its decay rate is – through the emission of Hawking radiation – and thus the shorter its lifetime. Astrophysical black holes with masses $M_{BH} \geq 3M_{\odot}$ emit radiation with an extremely small rate^a and their lifetime, given by the four-dimensional relation

$$\tau \sim \frac{1}{M_P} \left(\frac{M_{BH}}{M_P} \right)^3, \quad (11)$$

turns out to be much larger than the age of the universe. On the other hand, the same formula tells us that tiny black holes (as the ones that might have been created in the early universe in $D = 4$) have an extremely short life-time, due to their huge emission rate, and must have decayed and evaporated long time ago. However, for small black holes, the presence of extra dimensions modifies also their lifetime, and it is now given by¹¹²

$$\tau \sim \frac{1}{M_*} \left(\frac{M_{BH}}{M_*} \right)^{(n+3)/(n+1)}. \quad (12)$$

The appearance of the low energy scale M_* in Eq. (12), instead of M_P as in Eq. (11), leads to black hole lifetimes much longer than the one in four dimensions. Nevertheless, for black holes with masses in the area of a few TeV, the lifetime is still a tiny fraction of a second: for $M_{BH} = 5$ TeV, the lifetime ranges from 1.7×10^{-26} sec (for $n = 1$) to 0.5×10^{-26} sec (for $n = 7$), while for $M_{BH} = 10$ TeV, the corresponding lifetime interval is from 1.6×10^{-26} sec (for $n = 1$) to 1.2×10^{-26} sec (for $n = 7$).

^aIn addition, these black holes have a temperature much smaller than the one of the Cosmic Microwave Background Radiation, $T = 2.73$ K = 2.3×10^{-4} eV, therefore, they actually absorb radiation from their environment instead of emitting

Despite their short lifetime, the fact that these small black holes might be created during collisions on, or close to, the Earth's surface makes the possibility of their observation a more realistic prospect.

4. Evaporation of Higher-Dimensional Black Holes

The emission of Hawking radiation is in fact compatible with the well-known result of the Theory of General Relativity that nothing can escape from inside the horizon of a black hole. The Hawking radiation can be conceived as the creation of a virtual pair of particles just outside the horizon of the black hole: the particle with the positive energy escapes to infinity while the antiparticle (the one with the negative energy) falls into the BH, where it can exist as an ordinary particle. The spectrum of the Hawking radiation coming from a black hole with temperature T_H is a thermal one with an *almost* blackbody profile. The flux spectrum, i.e. the number of particles emitted per unit time, from a higher-dimensional spherically-symmetric black hole of the type (7), can be easily found by generalizing the corresponding four-dimensional expression¹¹⁴ for a higher number of dimensions. It is given by

$$\frac{dN^{(s)}(\omega)}{dt} = \sum_j \sigma_{j,n}^{(s)}(\omega) \frac{1}{\exp(\omega/T_H) \pm 1} \frac{d^{n+3}k}{(2\pi)^{n+3}}, \quad (13)$$

where s is the spin of the emitted degree of freedom and j its angular momentum quantum number. The spin statistics factor in the denominator is -1 for bosons and $+1$ for fermions. For massless particles, $|k| = \omega$ and the phase-space integral reduces to an integral over the energy of the emitted particle ω . For massive particles, $|k|^2 = \omega^2 - m^2$, and the energy in the denominator now includes the rest mass of the particle: this means that a black hole temperature $T_H \geq m$ is necessary for the emission of a particle with mass m . We should note here that, as the decay progresses, the black hole mass decreases and the Hawking temperature rises. It is usually assumed that a quasi-stationary approach to the decay is valid – that is, the black hole has time to come into equilibrium at each new temperature before the next particle is emitted. We will make this assumption also here.

The power spectrum, i.e. the energy emitted per unit time by the black hole, can be easily found by combining the number of particles emitted with the amount of energy they carry. It is given by

$$\frac{dE^{(s)}(\omega)}{dt} = \sum_j \sigma_{j,n}^{(s)}(\omega) \frac{\omega}{\exp(\omega/T_H) \pm 1} \frac{d^{n+3}k}{(2\pi)^{n+3}}. \quad (14)$$

Both expressions, Eqs. (13) and (14), contain an additional factor, $\sigma_{j,n}^{(s)}(\omega)$, which does not usually exist in a typical blackbody spectrum, or, more accurately, is just a constant standing for the area of the emitted body. In contrast, this factor here depends on the energy of the emitted particle, its spin and its angular momentum number. It may therefore significantly modify the spectrum of the emitted radiation and, for that reason, is called the ‘greybody’ factor. Equally important is the fact

that this coefficient depends also on the number of extra dimensions and therefore encodes valuable information for the structure of the spacetime around the black hole including the dimensionality of spacetime.

The distortion of the blackbody spectrum, or in other words, the presence of the greybody factor in the radiation spectrum of a black hole, can be attributed to the following fact: any particle emitted by a black hole has to traverse a strong gravitational background before reaching the observer at infinity, unlike to what happens with a black body in flat spacetime. The radiation spectrum is bound to depend on the energy of the propagating particle and the shape of the gravitational barrier as these are the parameters that will determine the number of particles that manage to reach infinity. In order to illustrate the above, let us assume, for example, that a scalar field of the form $\phi(t, r, \theta_i, \varphi) = e^{-i\omega t} R_{\omega\ell}(r) \tilde{Y}_\ell(\Omega)$, where $\tilde{Y}_\ell(\Omega)$ is the $(4+n)$ -dimensional generalization of the usual spherical harmonic functions¹¹⁵, propagates in the background of Eq. (7). Its radial equation of motion may then be written in a Schrödinger-like form

$$\left(-\frac{d^2}{dy^2} + r^{2n+4} \left[-\omega^2 + \frac{\ell(\ell+n+1)h(r)}{r^2} \right] \right) R_{\omega\ell}(y) = 0, \quad (15)$$

in terms of the ‘tortoise’ coordinate

$$y = \frac{\ln h(r)}{r_H^{n+1} (n+1)}, \quad \text{with} \quad h(r) = 1 - \left(\frac{r_H}{r} \right)^{n+1}. \quad (16)$$

The quantity inside square brackets in Eq. (15) gives the effective potential barrier in the area outside the horizon of the black hole. It clearly depends on all parameters mentioned above: ω , j (being equal to the orbital angular momentum number ℓ in the case of a scalar particle) and n . As a similar analysis will shortly show, it also depends on the value of the spin s , for a non-zero spin particle. By simple inspection, one may see that the barrier lowers for larger energy ω , while it rises for higher angular momenta ℓ – the dependence, however, on the number of extra dimensions is more subtle.

The greybody factor $\sigma_{j,n}^{(s)}(\omega)$ then stands for the corresponding transmission cross-section for a particle propagating in the aforementioned background. This quantity can be determined by solving the equation of motion of a given particle and computing the corresponding absorption coefficient $\mathcal{A}_j^{(s)}$. Then, we may write¹¹⁶

$$\sigma_{j,n}^{(s)}(\omega) = \frac{2^n \pi^{(n+1)/2} \Gamma[(n+1)/2]}{n! \omega^{n+2}} \frac{(2j+n+1)(j+n)!}{j!} |\mathcal{A}_j^{(s)}|^2. \quad (17)$$

It will be useful to rewrite the above expression for the greybody factor as

$$\sigma_{j,n}^{(s)}(\omega) = \frac{2^n}{\pi} \Gamma\left(\frac{n+3}{2}\right)^2 \frac{A_H}{(\omega r_H)^{n+2}} N_j |\mathcal{A}_j^{(s)}|^2, \quad (18)$$

where N_j is the multiplicity of states corresponding to the same partial wave j , given for a $(4+n)$ -dimensional spacetime by¹¹⁷

$$N_\ell = \frac{(2j+n+1)(j+n)!}{j!(n+1)!}, \quad (19)$$

and A_H is the horizon area of the $(4+n)$ -dimensional black hole defined as

$$\begin{aligned}
 A_H &= r_H^{n+2} \int_0^{2\pi} d\varphi \prod_{k=1}^{n+1} \int_0^\pi \sin^k \theta_{k+1} d\sin \theta_{k+1} \\
 &= r_H^{n+2} (2\pi) \prod_{k=1}^{n+1} \sqrt{\pi} \frac{\Gamma[(k+1)/2]}{\Gamma[(k+2)/2]} \\
 &= r_H^{n+2} (2\pi) \pi^{(n+1)/2} \Gamma\left(\frac{n+3}{2}\right)^{-1}.
 \end{aligned} \tag{20}$$

From Eq. (18), we may see that the greybody factor is indeed proportional to the area of the emitted body, as in the case of blackbody emission, nevertheless additional factors change, in principle, this simple relation by adding an explicit dependence on ω , r_H , j and n . We should also note that $\sigma_{j,n}^{(s)}(\omega)$ has the same dimensions as A_H , therefore its dimensionality changes as the number of extra dimensions n varies. Normalizing its expression to the area of the horizon of the $(4+n)$ -dimensional black hole would therefore be useful in comparing its values for different n .

Equation (14), for energy emission in the higher-dimensional spacetime, may take a simpler form when written in terms of the absorption coefficient. Then, it reads

$$\frac{dE^{(s)}(\omega)}{dt} = \sum_j N_j |\mathcal{A}_j^{(s)}|^2 \frac{\omega}{\exp(\omega/T_{BH}) \pm 1} \frac{d\omega}{2\pi}. \tag{21}$$

In the above, we have assumed that the emitted particles are massless, an assumption that will be made throughout this review. This simple, alternative form of the power spectrum has led part of the community to referring to the absorption probability $|\mathcal{A}_j^{(s)}|^2$ as the greybody factor, this however will not be followed here.

As we mentioned above the greybody factor modifies the spectrum of emitted particles from that of a perfect thermal blackbody¹¹⁴. Four-dimensional analyses for Schwarzschild^{118,119,120} and Kerr¹²¹ black holes have determined, both analytically and numerically, the greybody factors for particles of different spin. In the simplest case of a non-rotating, Schwarzschild black hole, geometric arguments show that, in the limit of high energy ω (the geometrical optics limit), $\sum_j \sigma_{j,n}^{(s)}(\omega)$ is a constant independent of ω ¹²² (for more details, see Sections 5 and 6). In that case, the spectrum is exactly like that of a blackbody for every particle species independently of their spin s . The low-energy behaviour, on the other hand, is strongly spin-dependent and energy-dependent, and the greybody factors are significantly different from the geometrical optics value^{118,120,123}. The result is that both the power and flux spectra peak at higher energies than those for a blackbody with the same temperature. Finally, the spin dependence of the greybody factors means that they are necessary to determine the relative emissivities of different particle types from a black hole.

For a charged black hole, early works^{124,125,126} showed that the black hole will quickly discharge through a Schwinger-type pair-production process. Moreover, the charge of the black hole could affect the geometry of spacetime and thus the emission of uncharged particles only for black holes with masses larger than $10^5 M_\odot$. A few years later, Page¹²⁷ showed that during the evaporation phase, the charge of the black hole fluctuates. The electrostatic potential between particle and antiparticle, together with the charge fluctuations, reduces the emitted flux and power of charged particles, bringing it down to 7% of the emission rate for similar but uncharged particles. In the same work, the effect of the rest mass m of the emitted particle was studied and found that it also reduces the emission rate: for electrons and muons, the reduction could be as large as 50% for black hole masses of $\mathcal{O}(10^{16} \text{ gr})$.

In the light of the recent speculations of the possible creation of higher-dimensional black holes during high-energy particle collisions, the generalization of the existing four-dimensional analyses for the calculation of greybody factors to a higher number of dimensions becomes imperative. On the one hand, the existence of extra dimensions might significantly change all that we know about the emission of particles from a black hole, including the rate of emission and the type of particles emitted. Moreover, if the dependence of the radiation spectrum on the dimensionality of spacetime is strong enough, then, a possible detection of such a spectrum can give us valuable information on the dimensionality of spacetime.

If, eventually, small higher-dimensional black holes may be created in high-energy particle collisions, then according to Refs. 69 and 72, the produced black holes will go through a number of phases before completely evaporating. These are:

- The *balding phase*: the black hole emits mainly gravitational radiation and sheds the ‘hair’ inherited from the original particles, and the asymmetry due to the violent production process.
- The *spin-down phase*: the typically non-zero impact parameter of the colliding partons leads to black holes with some angular momentum about an axis perpendicular to the plane. During this phase, the black hole loses its angular momentum through the emission of Hawking radiation and, possibly, through superradiance.
- The *Schwarzschild phase*: a spherically-symmetric black hole loses energy due to the emission of Hawking radiation. This results in the gradual decrease of its mass and the increase of its temperature.
- The *Planck phase*: the mass and/or the Hawking temperature approach M_* – a theory of quantum gravity is necessary to study this phase in detail.

An important question related to the aforementioned life stages of the black hole is how much energy is spent during each one of those phases. We have already seen how the initial four-dimensional estimate of 16% of the total energy emitted in the form of gravitational radiation during the balding phase, can go up to 55% depending on the value of the impact parameter and the dimensionality of spacetime. Crude estimates of the corresponding percentages in four dimensions give 25%

and 60% for the spin-down and Schwarzschild phase^{69,72}, respectively. However, it becomes clear that exact analyses performed in the higher-dimensional spacetime, in conjunction with the results derived already for the balding phase, can radically change those numbers.

In what follows, we will concentrate on the second and third phase of the life of the black hole, that is the spin-down and Schwarzschild phase. We will ignore the charge of the black hole: although we expect the aforementioned 7% figure, for the emission rate of charged particles, to change with the addition of extra dimensions, we anticipate that any increase would still allow us to ignore the emission of charged particles, at least at first approximation. We will also study the emission of only massless particles: the mass of the black hole, being in the trans-Planckian regime of a few TeV's, leads to temperatures that are much larger than the rest masses of all known particles (see Table 2).

Another comment is in order here: the presence of the brane has so far been ignored under the assumption that its tension is much smaller than the mass of the black hole and thus it does not change the gravitational background. Nevertheless, the brane plays another role, that of our four-dimensional world where, according to the assumptions of the Theories with Large Extra Dimensions, all ordinary particles (fermions, gauge bosons and Higgs fields) are localized. A $(4+n)$ -dimensional black hole emits Hawking radiation both in the bulk and on the brane. Since only gravitons, and possibly scalar fields, live in the bulk, these are the only particles that can be emitted in the bulk. On the other hand, the emission of brane-localized modes include zero-mode scalars, fermions, gauge bosons and zero-mode gravitons. From the observational point of view, it is much more interesting to study the emission of brane-localized modes, however, the emission in the bulk is equally important since it provides answers to questions like how much energy is available for emission of Standard Model particles on the brane.

The brane-localized modes and bulk modes live in spacetimes of different dimensionality. Whereas the bulk modes have access to the whole of the $(4+n)$ -dimensional spacetime, the brane modes live in a four-dimensional slice of it, which is the projection of the higher-dimensional spacetime on the brane. In order to study the emission of both types of modes, we need to write down the corresponding equations of motion of those fields. In the next section, we will first derive the *master equation* describing the motion of a field with arbitrary spin s in the background of a higher-dimensional Kerr-like black hole projected onto our brane; then, we will move on to review the so far derived results for the emission of Hawking radiation from rotating and non-rotating, uncharged $(4+n)$ -dimensional black holes on the brane. A similar review of the emission of Hawking radiation in the bulk is left for Section 6.

5. Master Equation and Hawking radiation on the Brane

The gravitational background around a $(4+n)$ -dimensional, rotating, uncharged black hole was found by Myers & Perry, and is given by the following line-element¹¹²

$$ds^2 = \left(1 - \frac{\mu}{\Sigma r^{n-1}}\right) dt^2 + \frac{2a\mu \sin^2 \theta}{\Sigma r^{n-1}} dt d\varphi - \frac{\Sigma}{\Delta} dr^2 - \Sigma d\theta^2 - \left(r^2 + a^2 + \frac{a^2\mu \sin^2 \theta}{\Sigma r^{n-1}}\right) \sin^2 \theta d\varphi^2 - r^2 \cos^2 \theta d\Omega_n, \quad (22)$$

where

$$\Delta = r^2 + a^2 - \frac{\mu}{r^{n-1}}, \quad \Sigma = r^2 + a^2 \cos^2 \theta, \quad (23)$$

and $d\Omega_n$ is the line-element on a unit n -sphere. The mass and angular momentum (transverse to the $r\varphi$ -plane) of the black hole are given by

$$M = \frac{(n+2)A_{n+2}}{16\pi G} \mu, \quad J = \frac{2}{n+2} Ma, \quad (24)$$

with G being the $(4+n)$ -dimensional Newton's constant, and A_{n+2} the area of a $(n+2)$ -dimensional unit sphere given by

$$A_{n+2} = \frac{2\pi^{(n+3)/2}}{\Gamma[(n+3)/2]}. \quad (25)$$

We will assume that the line-element (22) describes successfully a small, higher-dimensional black hole during its spin-down phase. At the end of this phase, the angular momentum will be lost, and the same line-element, in the limit $a \rightarrow 0$, will describe the following spherically-symmetric Schwarzschild phase of the life of the black hole. As mentioned earlier, in this section, we will be interested in the emission of Hawking radiation on the brane, therefore we need to determine the line-element in which the brane-localized modes propagate. This can be found by fixing the values of the additional angular coordinates describing the compact n dimensions, and, then, the induced-on-the-brane line-element is described again by Eq. (22) but with the last term omitted.

In order to derive a *master equation* describing the motion of a field with arbitrary spin s in the aforementioned projected background, we need to make use of the Newman-Penrose formalism^{128,129} that puts spinor calculus and gravitational quantities in the same framework. We first need to choose a tetrad basis of null vectors $(\ell^\mu, n^\mu, m^\mu, \bar{m}^\mu)$, where ℓ and n are real vectors, and m and \bar{m} are a pair of complex conjugate vectors. They satisfy the relations: $\mathbf{l} \cdot \mathbf{n} = 1$, $\mathbf{m} \cdot \bar{\mathbf{m}} = -1$, with all other products being zero. Such a tetrad basis is given below:

$$\ell^\mu = \left(\frac{r^2 + a^2}{\Delta}, 1, 0, \frac{a}{\Delta} \right), \quad n^\mu = \left(\frac{r^2 + a^2}{2\Sigma}, -\frac{\Delta}{2\Sigma}, 0, \frac{a}{2\Sigma} \right),$$

$$m^\mu = \left(ia \sin \theta, 0, 1, \frac{i}{\sin \theta} \right) \frac{1}{\sqrt{2}\bar{\rho}}, \quad \bar{m}^\mu = \left(-ia \sin \theta, 0, 1, \frac{-i}{\sin \theta} \right) \frac{1}{\sqrt{2}\bar{\rho}^*}, \quad (26)$$

where $\bar{\rho} = r + ia \cos \theta$. The λ_{abc} coefficients, which are used to construct the *spin coefficients*, are defined as:

$$\lambda_{abc} = (e_b)_{i,j} \left[(e_a)^i (e_c)^j - (e_a)^j (e_c)^i \right], \quad (27)$$

where e_a stands for each one of the null vectors and (i, j) denote the components of each vector. To determine λ_{abc} we will also need the expressions of the null vectors with their index down, and these are:

$$\begin{aligned} \ell_\mu &= \left(1, -\frac{\Sigma}{\Delta}, 0, -a \sin^2 \theta \right), & n_\mu &= \left(\frac{\Delta}{2\Sigma}, \frac{1}{2}, 0, -\frac{a \sin^2 \theta \Delta}{2\Sigma} \right), \\ m_\mu &= \left[ia \sin \theta, 0, -\Sigma, -i \sin \theta (r^2 + a^2) \right] \frac{1}{\sqrt{2}\bar{\rho}}, & \bar{m}_\mu &= (m_\mu)^*. \end{aligned} \quad (28)$$

Then, the non-vanishing components of the λ_{abc} coefficients are found to be:

$$\begin{aligned} \lambda_{122} &= -\frac{1}{\Sigma^2} \left(\frac{\Sigma}{2} \partial_r \Delta - r \Delta \right), & \lambda_{132} &= \frac{i\sqrt{2}a \sin \theta}{\Sigma \bar{\rho}}, & \lambda_{143} &= \frac{1}{\bar{\rho}}, \\ \lambda_{213} &= -\frac{\sqrt{2}a^2 \cos \theta \sin \theta}{\Sigma \bar{\rho}}, & \lambda_{243} &= -\frac{\Delta}{2\Sigma \bar{\rho}}, & \lambda_{314} &= -\frac{2ia \cos \theta}{|\bar{\rho}|^2}, \\ \lambda_{324} &= -\frac{ia \cos \theta \Delta}{\Sigma |\bar{\rho}|^2}, & \lambda_{334} &= \frac{r \cos \theta + ia}{\sqrt{2}\bar{\rho}^2 \sin \theta}. \end{aligned} \quad (29)$$

The above components must be supplemented by those that follow from the symmetry $\lambda_{abc} = -\lambda_{cba}$ and the complex conjugates obtained by replacing an index 3 by 4 (or vice versa) or interchanging 3 and 4 (when they are both present).

We may now compute the *spin coefficients* defined by $\gamma_{abc} = (\lambda_{abc} + \lambda_{cab} - \lambda_{bca})/2$. Particular components, or combinations, of the spin coefficients can be directly used in the field equations^{128,129}. These are found to have the values:

$$\begin{aligned} \kappa &= \sigma = \lambda = \nu = \epsilon = 0, & \rho &= -\frac{1}{\bar{\rho}^*}, & \mu &= -\frac{\Delta}{2\Sigma \bar{\rho}^*}, & \tau &= -\frac{ia \sin \theta}{\sqrt{2}\Sigma}, \\ \pi &= \frac{ia \sin \theta}{\sqrt{2}\bar{\rho}^{*2}}, & \gamma &= \frac{\partial_r \Delta}{4\Sigma} - \frac{\Delta}{2\Sigma \bar{\rho}^*}, & \beta &= \frac{\cot \theta}{2\sqrt{2}\bar{\rho}}, & \alpha &= \pi - \beta^*. \end{aligned} \quad (30)$$

In what follows, we will also employ the Newman-Penrose operators:

$$\begin{aligned} \hat{D} &= \frac{(r^2 + a^2)}{\Delta} \frac{\partial}{\partial t} + \frac{\partial}{\partial r} + \frac{a}{\Delta} \frac{\partial}{\partial \varphi}, \\ \hat{\Delta} &= \frac{(r^2 + a^2)}{2\Sigma} \frac{\partial}{\partial t} - \frac{\Delta}{2\Sigma} \frac{\partial}{\partial r} + \frac{a}{2\Sigma} \frac{\partial}{\partial \varphi}, \\ \hat{\delta} &= \frac{1}{\sqrt{2}\bar{\rho}} \left(ia \sin \theta \frac{\partial}{\partial t} + \frac{\partial}{\partial \theta} + \frac{i}{\sin \theta} \frac{\partial}{\partial \varphi} \right), \end{aligned} \quad (31)$$

and make use of the following field factorization:

$$\Psi_s(t, r, \theta, \varphi) = e^{-i\omega t} e^{im\varphi} R_s(r) S_{s,j}^m(\theta), \quad (32)$$

where $S_{s,j}^m(\theta)$ are the so-called spin-weighted spheroidal harmonics. For $s = 0$, these angular eigenfunctions reduce to the spheroidal harmonics¹³⁰, while for $a\omega = 0$, they take the form of the spin-weighted spherical harmonics¹³¹. In what follows, we will address separately the equation of motion of each type of field (gauge bosons, fermions and scalars) in the background of the projected, Kerr-like black hole.

Gauge Bosons ($s = 1$). In the Newman-Penrose formalism, there are only three ‘degrees of freedom’ for a gauge field, namely $\Phi_0 = F_{13}$, $\Phi_1 = (F_{12} + F_{43})/2$ and $\Phi_2 = F_{42}$, in terms of which the different components of the Yang-Mills equation for a massless gauge field are written as:

$$(\hat{D} - 2\rho) \Phi_1 - (\hat{\delta}^* + \pi - 2\alpha) \Phi_0 = 0, \quad (33)$$

$$(\hat{\delta} - 2\tau) \Phi_1 - (\hat{\Delta} + \mu - 2\gamma) \Phi_0 = 0, \quad (34)$$

$$(\hat{D} - \rho) \Phi_2 - (\hat{\delta}^* + 2\pi) \Phi_1 = 0, \quad (35)$$

$$(\hat{\delta} - \tau + 2\beta) \Phi_2 - (\hat{\Delta} + 2\mu) \Phi_1 = 0, \quad (36)$$

where $\hat{\delta}^*$ stands for the complex conjugate of $\hat{\delta}$. One of the main difficulties in writing down equations of motion for fields with a non-zero spin, and thus with more than one components, is to decouple the differential equation for a particular component from the remaining ones. This is not always possible but for the axially-symmetric Kerr-like black hole that we consider here it is. The situation actually is very similar to the pure four-dimensional case studied by Teukolsky¹³², where it was shown that at least the radiative components, that carry all the information for the propagating field, do indeed decouple¹³³. Rearranging Eqs. (33)-(34) and using the identity

$$(\hat{D} - 2\rho - \rho^*)(\hat{\delta} - 2\tau) \Phi_1 = (\hat{\delta} - 2\tau)(\hat{D} - 2\rho) \Phi_1, \quad (37)$$

we obtain the following decoupled equation for Φ_0

$$(\hat{D} - 2\rho - \rho^*)(\hat{\Delta} + \mu - 2\gamma) \Phi_0 - (\hat{\delta} - 2\tau)(\hat{\delta}^* + \pi - 2\alpha) \Phi_0 = 0. \quad (38)$$

Using the explicit forms of spin coefficients and operators, Eqs. (30) and (31), as well as the factorized ansatz (32), the above can be conveniently separated into an angular equation,

$$\begin{aligned} \frac{1}{\sin \theta} \frac{d}{d\theta} \left(\sin \theta \frac{dS_{1,j}^m}{d\theta} \right) + \left[-\frac{2m \cot \theta}{\sin \theta} - \frac{m^2}{\sin^2 \theta} + a^2 \omega^2 \cos^2 \theta \right. \\ \left. - 2a\omega \cos \theta + 1 - \cot^2 \theta + \lambda_{1j} \right] S_{1,j}^m(\theta) = 0, \end{aligned} \quad (39)$$

where λ_{1j} is a separation constant, and a radial equation,

$$\frac{1}{\Delta} \frac{d}{dr} \left(\Delta^2 \frac{dR_1}{dr} \right) + \left[\frac{K^2 - iK\partial_r \Delta}{\Delta} + 4i\omega r + (\Delta'' - 2) - \Lambda_{1j} \right] R_1(r) = 0, \quad (40)$$

where we have defined:

$$K = (r^2 + a^2)\omega - am, \quad \Lambda_{sj} = \lambda_{sj} + a^2\omega^2 - 2am\omega. \quad (41)$$

Fermion Fields ($s = 1/2$). For a massless two-component spinor field, the Dirac equation can be written as:

$$(\hat{\delta}^* - \alpha + \pi)\chi_0 = (\hat{D} - \rho)\chi_1, \quad (42)$$

$$(\hat{\Delta} + \mu - \gamma)\chi_0 = (\hat{\delta} + \beta - \tau)\chi_1. \quad (43)$$

Performing a similar rearrangement as in the case of bosons and using the identity

$$(\hat{\delta} - \alpha^* - \tau + \pi^*)(\hat{D} - \rho)\chi_1 = (\hat{D} - \rho - \rho^*)(\hat{\delta} + \beta - \tau)\chi_1, \quad (44)$$

we find that χ_1 is decoupled leaving behind an equation for χ_0

$$(\hat{D} - \rho - \rho^*)(\hat{\Delta} + \mu - \gamma)\chi_0 - (\hat{\delta} - \alpha^* - \tau + \pi^*)(\hat{\delta}^* - \alpha + \pi)\chi_0 = 0. \quad (45)$$

The latter can be explicitly written as a set of angular and radial equations, having the form

$$\begin{aligned} \frac{1}{\sin \theta} \frac{d}{d\theta} \left(\sin \theta \frac{dS_{1/2,j}^m}{d\theta} \right) + \left[-\frac{m \cot \theta}{\sin \theta} - \frac{m^2}{\sin^2 \theta} + a^2 \omega^2 \cos^2 \theta \right. \\ \left. - a \omega \cos \theta + \frac{1}{2} - \frac{1}{4} \cot^2 \theta + \lambda_{\frac{1}{2}j} \right] S_{1/2,j}^m(\theta) = 0, \end{aligned} \quad (46)$$

and

$$\frac{1}{\sqrt{\Delta}} \frac{d}{dr} \left(\Delta^{3/2} \frac{dR_{1/2}}{dr} \right) + \left[\frac{K^2 - iK(\partial_r \Delta)/2}{\Delta} + 2i\omega r + \frac{1}{2}(\Delta'' - 2) - \Lambda_{\frac{1}{2}j} \right] R_{1/2}(r) = 0, \quad (47)$$

respectively, with the same definitions for K and Λ_{sj} as before.

Scalar Fields ($s = 0$). In the case of a scalar field, its equation of motion can be determined quite easily by evaluating the double covariant derivative $g^{\mu\nu} D_\mu D_\nu$ acting on the field. As in the purely four-dimensional case ¹³⁴, the use of the factorized ansatz (32) leads, similarly to the previous cases, to the following pair of separated equations

$$\frac{1}{\sin \theta} \frac{d}{d\theta} \left(\sin \theta \frac{dS_{0,\ell}^m}{d\theta} \right) + \left[-\frac{m^2}{\sin^2 \theta} + a^2 \omega^2 \cos^2 \theta + \lambda_{0\ell} \right] S_{0,\ell}^m = 0, \quad (48)$$

$$\frac{d}{dr} \left(\Delta \frac{dR_0}{dr} \right) + \left(\frac{K^2}{\Delta} - \Lambda_{0\ell} \right) R_0(r) = 0, \quad (49)$$

where $Y_{0,\ell}^m = e^{im\varphi} S_{0,\ell}^m(\theta)$ are now the spheroidal wave functions ¹³⁰.

Combining all the above equations derived for bosons, fermions and scalar fields, we may now rewrite them in the form of a *master equation* valid for all types of fields. The radial equation then takes the form:

$$\Delta^{-s} \frac{d}{dr} \left(\Delta^{s+1} \frac{dR_s}{dr} \right) + \left(\frac{K^2 - isK\partial_r\Delta}{\Delta} + 4is\omega r + s(\Delta'' - 2) - \Lambda_{sj} \right) R_s(r) = 0, \quad (50)$$

while, the angular equation reads

$$\frac{1}{\sin\theta} \frac{d}{d\theta} \left(\sin\theta \frac{dS_{s,j}^m}{d\theta} \right) + \left[-\frac{2ms\cot\theta}{\sin\theta} - \frac{m^2}{\sin^2\theta} + a^2\omega^2\cos^2\theta - 2as\omega\cos\theta - s^2\cot^2\theta + \lambda_{sj} \right] S_{s,j}^m = 0. \quad (51)$$

The latter equation is identical to the one derived by Teukolsky¹³² in the case of a rotating, Kerr black hole. The radial equation differs by the extra factor $s(\Delta'' - 2)$ due to the fact that for our metric tensor this combination is not zero, contrary to what happens in the case of the 4-dimensional Kerr, or Schwarzschild, metric.

In order to solve the radial equation (50), we need to know the value of the constant term Λ_{sj} defined in Eq. (41), or alternatively the value of the separation constant λ_{sj} that appears in the angular equation (51). Actually, the separability of radial and angular parts in the equation of motion of a field in a Kerr-like black hole background comes with a price: the separation constant is a complicated function of both the energy ω of the particle and the angular momentum parameter a of the black hole. An analytic form can be found, for any value of s , in the limit of $a\omega \rightarrow 0$, in which case we may write^{135,136,137}

$$\lambda_{sj} = -s(s+1) + \sum_k f_k^{jms}(a\omega)^k = j(j+1) - s(s+1) - \frac{2ms^2}{j(j+1)} a\omega + \dots, \quad (52)$$

where terms higher than linear have been suppressed due to their complexity. It becomes therefore clear that any attempt to solve analytically the radial equation (50) must necessarily take place in the low-energy and low-momentum limit.

Finally, we may simplify further the radial equation (50) by making the redefinition $R_s = \Delta^{-s} P_s$. In that case, the Δ'' -term disappears and we obtain:

$$\Delta^s \frac{d}{dr} \left(\Delta^{1-s} \frac{dP_s}{dr} \right) + \left(\frac{K^2 - isK\partial_r\Delta}{\Delta} + 4is\omega r - \tilde{\Lambda}_{sj} \right) P_s(r) = 0, \quad (53)$$

where now $\tilde{\Lambda}_{sj} = \Lambda_{sj} + 2s$.

Having derived the equation of motion for fields with arbitrary spin s propagating in the four-dimensional spacetime induced on the 3-brane, we can now move on to discuss the emission of Hawking radiation directly on the brane during the spin-down and Schwarzschild phase of a small, higher-dimensional black hole.

5.1. Emission of Hawking radiation during the spin-down phase

The study of the emission of Hawking radiation on the brane during the spin-down phase has not been as thorough as one would hope. The only such attempt has been made by the authors of Ref. 67, who independently performed the derivation of the *master equation* described earlier ^b. The master equation was solved analytically in the limit of small $a\omega$ and for the particular case of only one extra compact dimension, i.e. $n = 1$. A well-known approximation method ^{135,118,119,120,138–146} was used according to which the asymptotic solutions at infinity and close to the horizon are found, and then matched in an intermediate zone in order to construct the complete analytic solution. The same method had been used earlier in Ref. 147 to compute the spectrum of Hawking radiation of scalar fields emitted both on the brane and in the bulk, and later, in Ref. 148, for the study of the emission of fermions and gauge bosons on the brane; both analyses were done for the Schwarzschild phase of the black hole, therefore, a description of the aforementioned approximation method will be given in the next subsection.

In Ref. 67, the greybody factors, as well as the radiation spectra, for the emission of scalars, fermions and gauge bosons on the brane during the spin-down phase were derived for $n = 1$. For various values of the angular momentum parameter a , the radiation spectra were plotted as a function of the energy ω of the emitted particle. The presented results reveal a suppression of the power spectrum for scalar fields, as the black hole angular momentum increases, both at low and high energies. On the other hand, in the radiation spectra for fermions and gauge bosons, we observe an enhancement at low energies that turns to a suppression at high energies. In all cases, the power emission curves, for all values of a and s , lie far below the ones produced by using the high-energy geometrical optics limit value of the greybody factors.

However, these analytic results were derived in the limit of small $a\omega$, therefore, they are bound to break down at high energies. The high energy behaviour of the power spectra presented are thus not trustable and an exact (numerical) analysis is necessary to determine the complete spectrum. By comparing the results, for $a = 0$ and $n = 1$, produced in Ref. 67 with the ones derived in the four-dimensional case ¹¹⁸, we conclude that the power spectrum of all fields seems to be enhanced. However, for $a > 0$, the suppression caused by the black hole angular momentum complicates the picture and the comparison with the four-dimensional case is not clear. Similarly, no conclusions can be drawn on the behaviour of the radiation spectra as n increases. Apart from an exact analysis, valid at all energy regimes, a complete study of the dependence of the emission spectra on the number of extra di-

^bA typographical error appears in the published version of Ref. 67: the coefficient s that should have multiplied the Δ'' -term [or $n(n-1)\mu r^{n-1}$, in their notation] is constantly missing from their equations for scalars (A5), fermions (A23) and gauge bosons (A26), as well as from the master equation (A28). Nevertheless, the results presented in Ref. 67 are still robust since they were derived for the particular case of $n = 1$ for which this term vanishes trivially.

mensions, is clearly necessary. Both of these tasks have been successfully performed in the case of the Schwarzschild phase¹⁴⁹, and the results are reviewed in the next subsection.

5.2. Emission of Hawking radiation during the Schwarzschild phase

In the four-dimensional case, the most optimistic estimates for the amount of the initial energy of the colliding particles lost in the balding ($\sim 16\%$) and spin-down ($\sim 25\%$) phases leave behind approximately 60% of the total energy to be spent during emission of Hawking radiation in the Schwarzschild phase. Although we now know that these numbers change with the addition of extra dimensions, we believe that the Schwarzschild phase will still be the longer one and will account for the greatest proportion of the mass loss in the life of a small, higher-dimensional black hole. Contrary to the case of the spin-down phase, the emission of Hawking radiation on the brane during the Schwarzschild phase has been thoroughly studied, both analytically^{147,148} and numerically¹⁴⁹. In what follows we present a review of both types of results (see also¹⁵⁰).

A higher-dimensional black hole with vanishing angular momentum induces on the 3-brane the following spherically-symmetric, Schwarzschild-like line-element

$$ds^2 = -h(r) dt^2 + h(r)^{-1} dr^2 + r^2 (d\theta^2 + \sin^2 \theta d\varphi^2), \quad (54)$$

where still

$$h(r) = 1 - \left(\frac{r_H}{r} \right)^{n+1}. \quad (55)$$

The above line-element follows easily from the one in Eq. (22) after projecting out the extra angular coordinates, by fixing their values, and then setting $a = 0$. As in the case of the projection of a Kerr-like line-element on the brane, the induced metric still has an explicit dependence on the number of extra dimensions that exist in the fundamental, higher-dimensional theory.

The master equation (53) also takes now a much more simplified form, namely

$$\Delta^s \frac{d}{dr} \left(\Delta^{1-s} \frac{dP_s}{dr} \right) + \left[\frac{\omega^2 r^2}{h} + 2i\omega sr - \frac{i\omega r^2 h'}{h} - \Lambda \right] P_s(r) = 0 \quad (56)$$

where now $\Lambda \equiv \tilde{\Lambda}_{sj} = j(j+1) - s(s-1)$. The above equation needs to be solved over the whole radial domain. We will first review the results that follow from the analytic approach^{147,148} and then move on to discuss the ones following from the numerical analysis¹⁴⁹.

As mentioned in the previous subsection, the analytic treatment demands the use of an approximate method in which the above equation is solved at the near-horizon regime ($r \simeq r_H$) and far-field regime ($r \gg r_H$), and the corresponding solutions are matched at an intermediate zone. In solving analytically Eq. (56), the spin s will remain an arbitrary parameter of the differential equation; this will allow us to solve the radial equation for particles with different spin s in a unified way.

Starting from the near-horizon (NH) regime, a change of variable $r \rightarrow h(r)$ brings Eq. (56) to the form ¹⁴⁸

$$h(1-h) \frac{d^2 P_s}{dh^2} + \left[(1-s)(1-h) - \frac{(n+2s)}{(n+1)} h \right] \frac{dP_s}{dh} + \left[\frac{(\omega r_H)^2}{(n+1)^2 h(1-h)} + \frac{2is\omega r_H - \Lambda}{(n+1)^2(1-h)} - \frac{is\omega r_H}{(n+1)h} \right] P_s = 0. \quad (57)$$

In the above, we have made use of the relation

$$\frac{dh}{dr} = \frac{(n+1)}{r} (1-h), \quad (58)$$

that follows from the definition (55). Making a further redefinition of the radial function, $P_s(h) = h^\alpha(1-h)^\beta F_s(h)$, the above equation takes the form of a hypergeometric equation for the radial function F_s , i.e.

$$h(1-h) \frac{d^2 F_s}{dh^2} + [c - (1+a+b)h] \frac{dF_s}{dh} - ab F_s = 0. \quad (59)$$

The hypergeometric indices (a, b, c) can be identified as

$$a = \alpha + \beta + \frac{s+n(1-s)}{(n+1)}, \quad b = \alpha + \beta, \quad c = 1 - s + 2\alpha. \quad (60)$$

The power coefficients α and β , in turn, are found by solving second-order algebraic equations leading to the results

$$\alpha_+ = s + \frac{i\omega r_H}{n+1}, \quad \alpha_- = -\frac{i\omega r_H}{n+1}, \quad (61)$$

and

$$\beta_\pm = \frac{1}{2(n+1)} \left[1 - 2s \pm \sqrt{(1+2j)^2 - 4\omega^2 r_H^2 - 8is\omega r_H} \right], \quad (62)$$

respectively. Then, by using the general solution ¹⁵¹ of the hypergeometric equation (59), together with the aforementioned relation between $P_s(h)$ and $F_s(h)$, we obtain the following general solution for the radial function $P_s(h)$ in the near-horizon regime:

$$P_{NH}(h) = A_- h^\alpha (1-h)^\beta F(a, b, c; h) + A_+ h^{-\alpha} (1-h)^\beta F(a-c+1, b-c+1, 2-c; h), \quad (63)$$

where A_\pm are arbitrary constants. For simplicity, in the above, we have dropped the spin index s from the radial function P .

An important boundary condition must be imposed on the general solution (63) at the horizon of the black hole: since nothing can escape from the black hole, in the limit $r \rightarrow r_H$ the above general solution must contain only incoming modes. In order to impose this condition, we expand Eq. (63) in the limit $r \rightarrow r_H$, or equivalently $h \rightarrow 0$, and we obtain

$$P_{NH} \simeq A_- h^\alpha + A_+ h^{-\alpha} = A_- h^s \exp(i\omega r_H^{n+2} y) + A_+ h^{-s} \exp(-i\omega r_H^{n+2} y) \quad (64)$$

for $\alpha = \alpha_+$, and

$$P_{NH} \simeq A_- \exp(-i\omega r_H^{n+2} y) + A_+ \exp(i\omega r_H^{n+2} y) \quad (65)$$

for $\alpha = \alpha_-$. In the above, we have used the ‘tortoise’ coordinate y defined in Eq. (16). The aforementioned boundary condition at the horizon demands that $A_- = 0$, in the former case, and $A_+ = 0$, in the latter case. However, the remaining term in the asymptotic solution for $\alpha = \alpha_+$ then describes an incoming wave with a diverging amplitude at the horizon. This is clearly an irregular solution, therefore the choice $\alpha = \alpha_+$ must be discarded altogether. On the other hand, the choice $\alpha = \alpha_-$ leads to a regular incoming wave with amplitude unity at the horizon. Finally, we need to make a choice for the sign appearing in the expression of the β coefficient. One can easily see that the criterion for the convergence of the hypergeometric function $F(a, b, c; h)$, i.e. $\mathbf{Re}(c - a - b) > 0$, clearly demands that we choose $\beta = \beta_-$.

Having found the solution in the near-horizon regime, we now turn our attention to the far-field asymptotic regime. In the limit $r \gg r_H$, or $h \rightarrow 1$, Eq. (56) assumes a simplified form, which reads¹⁴⁸

$$\frac{d^2 P}{dr^2} + \frac{2(1-s)}{r} \frac{dP}{dr} + \left(\omega^2 + \frac{2is\omega}{r} - \frac{\Lambda}{r^2} \right) P = 0. \quad (66)$$

Another redefinition of the radial function, $P = e^{-i\omega r} r^{j+s} \tilde{P}(r)$, and a change of variable, $z = 2i\omega r$, puts the above equation in the form of a confluent hypergeometric equation

$$z \frac{d^2 \tilde{P}}{dz^2} + (b - z) \frac{d\tilde{P}}{dz} - a\tilde{P} = 0, \quad (67)$$

with $a = j - s + 1$ and $b = 2j + 2$. The general solution of the above differential equation is given by¹⁵¹

$$\tilde{P}(z) = B_+ M(a, b, z) + B_- U(a, b, z), \quad (68)$$

where M and U are the Kummer functions, and B_\pm are arbitrary coefficients. Then, the complete solution for the radial function $P(r)$ at $r \gg r_H$ can be written as

$$P_{FF}(r) = e^{-i\omega r} r^{j+s} \left[B_+ M(j - s + 1, 2j + 2, 2i\omega r) + B_- U(j - s + 1, 2j + 2, 2i\omega r) \right]. \quad (69)$$

In order to construct a complete solution for the radial function $P(r)$, we need to match the two asymptotic solutions at an intermediate zone. Although they look different, we will see that they actually take a very similar form in the intermediate regime, which facilitates considerably their matching. In order to see that, we first shift the hypergeometric function towards large values of r . This can be done by using a standard linear transformation formula^{148,151}, that changes its argument

from h to $1 - h$. Then, expanding in the limit $r \rightarrow \infty$, or $h \rightarrow 1$, we obtain ^c

$$\begin{aligned} P_{NH}(h) \simeq & A_- \left(\frac{r}{r_H} \right)^{j+s} \frac{\Gamma(1-s+2\alpha) \Gamma(-2\beta + \frac{1-2s}{n+1})}{\Gamma(\alpha-\beta+1-s) \Gamma(\alpha-\beta+\frac{1-2s}{n+1})} \\ & + A_- \left(\frac{r_H}{r} \right)^{j-s+1} \frac{\Gamma(1-s+2\alpha) \Gamma(2\beta - \frac{1-2s}{n+1})}{\Gamma(\alpha+\beta) \Gamma(\alpha+\beta+\frac{s+n(1-s)}{n+1})}. \end{aligned} \quad (70)$$

We then expand the far-field solution (69) in the limit $\omega r \ll 1$, and we take

$$P_{FF}(r) = B_+ r^{j+s} + \frac{B_-}{r^{j-s+1}} \frac{\Gamma(2j+1)}{\Gamma(j-s+1) (2i\omega)^{2j+1}}. \quad (71)$$

The matching of the two solutions (70) and (71) clearly provides relations between the integration constants appearing in the expressions of the asymptotic solutions. These read

$$B_+ = \frac{A_-}{r_H^{j+s}} \frac{\Gamma(1-s+2\alpha) \Gamma(-2\beta + \frac{1-2s}{n+1})}{\Gamma(\alpha-\beta+1-s) \Gamma(\alpha-\beta+\frac{1-2s}{n+1})}, \quad (72)$$

$$B_- = \frac{A_- r_H^{j-s+1} (2i\omega)^{2j+1} \Gamma(1-s+2\alpha) \Gamma(2\beta - \frac{1-2s}{n+1}) \Gamma(j-s+1)}{\Gamma(\alpha+\beta) \Gamma(\alpha+\beta+\frac{s+n(1-s)}{n+1}) \Gamma(2j+1)}. \quad (73)$$

The above relations complete the determination of the solution for the radial function $P_s(r)$ that describes the propagation of scalars, fermions and gauge-bosons in the background of a projected $(4+n)$ -dimensional Schwarzschild-like black hole on a 4-dimensional brane.

We may now proceed to the calculation of the greybody factors for each type of field. For this, we need the amplitudes of the incoming and outgoing modes at infinity. This can be found by taking the limit $r \rightarrow \infty$ of the far-field solution (69). Then, we obtain

$$P_s^{(\infty)}(r) = A_{in}^{(\infty)} \frac{e^{-i\omega r}}{(2\omega r)^{1-2s}} + A_{out}^{(\infty)} \frac{e^{i\omega r}}{(2\omega r)} + \dots \quad (74)$$

with

$$A_{in}^{(\infty)} = \frac{e^{-i\pi(j-s+1)/2}}{(2\omega)^{j+s}} \left[B_- + \frac{B_+ e^{i\pi(j-s+1)} \Gamma(2j+2)}{\Gamma(j+s+1)} \right], \quad (75)$$

$$A_{out}^{(\infty)} = \frac{B_+ e^{-i\pi(j-s+1)/2} \Gamma(2j+2)}{\Gamma(j-s+1) (2\omega)^{j+s}}. \quad (76)$$

^cIn order to obtain the simple powers of r shown in the expression below, the low-energy limit, $\omega r_H \ll 1$, has been taken in the expression of the β coefficient in the first term of Eq. (63). No expansion has been made in the arguments of the Gamma functions.

A few comments are here in order: for $s = 0$, the above expression describes the incoming and outgoing mode of a scalar field at infinity, both scaling as $1/r$; this expression, therefore, contains the complete information for the propagating scalar field and the two amplitudes, $A_{in}^{(\infty)}$ and $A_{out}^{(\infty)}$, can be used to determine the reflection coefficient \mathcal{R} , and from that the absorption coefficient \mathcal{A} , as follows

$$|\mathcal{A}_j^{(0)}|^2 = 1 - |\mathcal{R}_j^{(0)}|^2 = 1 - \left| \frac{A_{out}^{(\infty)}}{A_{in}^{(\infty)}} \right|^2, \quad (77)$$

On the other hand, for $s \neq 0$ and $s = +|s|$, Eq. (74) describes a dominant incoming mode and a suppressed outgoing one; vice versa, for $s = -|s|$, the outgoing mode dominates while the incoming one is greatly suppressed. This is merely a reflection of the fact that, for $s \neq 0$, the propagating field has more than one components, each one of which mainly describes either the incoming mode or the outgoing mode. What is fortunate is that we do not need to know the complete solution at infinity as long as we can compute the total incoming flux \mathcal{F}_{in} at the horizon and at infinity. Then, the absorption coefficient may be directly determined through the following expression

$$|\mathcal{A}_j^{(s)}|^2 = \frac{\mathcal{F}_{in}^{(h)}}{\mathcal{F}_{in}^{(\infty)}}. \quad (78)$$

The calculation of the incoming flux is indeed possible for the spherically-symmetric Schwarzschild-like background that we consider here^d, so the only component whose expression we need to calculate, for fields with a non-zero spin, is the upper one, with $s = +|s|$.

The incoming flux of a fermionic field can be computed from the radial component of the conserved current, $J^\mu = \sqrt{2} \sigma_{AB}^\mu \psi^A \bar{\psi}^B$, integrated over a two-dimensional sphere, first at infinity and then at the horizon^{145,148}. For gauge bosons, the (tr) -component of the energy momentum tensor $T^{\mu\nu} = 2\sigma_{AA'}^\mu \sigma_{BB'}^\nu \psi^{AB} \bar{\psi}^{A'B'}$ can be used instead. The same method for the calculation of the absorption coefficient can be equally well applied also in the case of a scalar field with the use of the radial component of the conserved current $J^\mu = hr^2 (\psi \partial^\mu \psi^* - \psi^* \partial^\mu \psi)$ - this method is completely equivalent to the one described above, that makes use of the expression of the reflection coefficient, while it allows us to write down a unified expression for the absorption probability for fields with arbitrary spin. Substituting the results for the incoming fluxes in Eq. (78), we may finally write

$$|\mathcal{A}_j^{(s)}|^2 = (2\omega r_H)^{2(1-2s)} \left| \frac{A_{in}^{(h)}}{A_{in}^{(\infty)}} \right|^2. \quad (79)$$

^dNote that for more complicated gravitational backgrounds, the calculation of the flux can be highly non-trivial, especially close to the horizon. In that case, the complete solution (both incoming and outgoing modes) at infinity must be determined.

where $A_{in}^{(h)} = A_-$, and $A_{in}^{(\infty)}$ is given in Eq. (75). In the above, we have taken into account the fact that, for fermions and gauge fields, the lower component contributes little to the in-falling flux both at infinity and at the horizon. We should note here that the coefficient in front of the ratio of the two amplitudes strongly depends on the field normalization (74) at infinity - although this is merely a convention, care should be taken so that this coefficient correctly reflects the chosen normalization ^e.

Substituting the expression of $A_{in}^{(\infty)}$ in Eq. (79) and using the relations (72) and (73), we obtain (for more information on the mathematical details omitted below, see Ref. 148)

$$|\mathcal{A}_j^{(s)}|^2 = \frac{(2\omega r_H)^{2j+2-2s}}{|\Gamma(1-s+2\alpha)|^2 |C(\omega r_H)^{2j+1} + D|^2}, \quad (80)$$

where the coefficients C and D stand for

$$C = \frac{2^{2j+1} e^{i\pi(s-1/2)} \Gamma\left(2\beta - \frac{1-2s}{n+1}\right) \Gamma(j-s+1)}{\Gamma(\alpha+\beta) \Gamma\left(\alpha+\beta + \frac{s+n(1-s)}{n+1}\right) \Gamma(2j+1)}, \quad (81)$$

$$D = \frac{\Gamma(2j+2) \Gamma\left(-2\beta + \frac{1-2s}{n+1}\right)}{\Gamma(\alpha-\beta+1-s) \Gamma\left(\alpha-\beta + \frac{1-2s}{n+1}\right) \Gamma(j+s+1)}. \quad (82)$$

Since we study the emission of brane-localized modes, this is clearly a four-dimensional process, therefore the relation (17) [or (18)] between the greybody factor and the absorption probability takes the simplified form

$$\sigma_{j,n}^{(s)}(\omega) = \frac{\pi}{\omega^2} (2j+1) |\mathcal{A}_j^{(s)}|^2 = \frac{A_H}{(2\omega r_H)^2} (2j+1) |\mathcal{A}_j^{(s)}|^2, \quad (83)$$

where $A_H = 4\pi r_H^2$, or finally

$$\sigma_{j,n}^{(s)}(\omega) = \frac{(2\omega r_H)^{2j-2s} (2j+1) A_H}{|\Gamma(1-s+2\alpha)|^2 |C(\omega r_H)^{2j+1} + D|^2}. \quad (84)$$

The coefficients C and D in the above expression depend, through Gamma functions, on the parameters of the theory, therefore the dependence of the greybody factor on the spin s , the energy ω , or the number of extra dimensions n is not clear. Nevertheless, the above expression can be easily plotted and thus reveal the desired dependence. Before however discussing those results, we might attempt to derive some simple, elegant expressions for the greybody factor by taking the low-energy limit $\omega r_H \ll 1$. In this limit, we may express each one of the coefficients C and D as a power series in (ωr_H) and keep only the leading term. Then, we may see ¹⁴⁸ that the term proportional to C , in the denominator of Eq. (84), is sub-dominant compared to the one proportional to D - that comes out to be independent of (ωr_H)

^eFor this reason, different coefficients appear in the expressions of the absorption probabilities $|\mathcal{A}_j^{(s)}|^2$ in Refs. 148 and 149, where different normalizations for the field at infinity were used.

at leading order – and thus the former can be ignored. Depending on the spin of the particle, additional powers of (ωr_H) may come from the measure of the remaining Gamma function in the denominator of Eq. (84). While for scalars and fermions, the zeroth-order term is (ωr_H) -independent, i.e.

$$\frac{1}{|\Gamma(1+2\alpha)|^2} = 1 + \frac{2\pi^2(\omega r_H)^2}{3(n+1)^2} + \mathcal{O}(\omega r_H)^4, \quad (85)$$

$$\frac{1}{|\Gamma(1/2+2\alpha)|^2} = \frac{1}{\pi} + \frac{2\pi(\omega r_H)^2}{(n+1)^2} + \mathcal{O}(\omega r_H)^4, \quad (86)$$

for gauge bosons this is not the case and extra powers of (ωr_H) come up

$$\frac{1}{\Gamma(2\alpha)\Gamma(-2\alpha)} = \frac{4(\omega r_H)^2}{(n+1)^2} + \mathcal{O}(\omega r_H)^4. \quad (87)$$

Putting everything together, we obtain the following simplified, low-energy expressions for the greybody factors

$$\sigma_{j,n}^{(0)}(\omega) = \frac{\pi(2j+1)}{(n+1)^2} \frac{\Gamma(\frac{j+1}{n+1})^2 \Gamma(1+\frac{j}{n+1})^2}{\Gamma(\frac{1}{2}+j)^2 \Gamma(1+\frac{2j+1}{n+1})^2} \left(\frac{\omega r_H}{2}\right)^{2j} A_H + \dots, \quad (88)$$

for scalars,

$$\sigma_{j,n}^{(1/2)}(\omega) = \frac{\pi(2j+1)2^{-(4j+2)/(n+1)}}{4\Gamma(j+1)^2} \left(\frac{\omega r_H}{2}\right)^{2j-1} A_H + \dots, \quad (89)$$

fermions,

$$\sigma_{j,n}^{(1)}(\omega) = \frac{(2j+1)}{(n+1)^2} \left(\frac{\Gamma(\frac{j}{n+1}) \Gamma(\frac{j+1}{n+1}) \Gamma(j+2)}{\Gamma(\frac{2j+1}{n+1}) \Gamma(2j+2)} \right)^2 (2\omega r_H)^{2j} A_H + \dots, \quad (90)$$

and gauge bosons. By choosing different values for $j \geq s$, the above approximate expressions reveal that, at the low-energy regime, the greybody factor for all types of fields gets suppressed as the angular momentum number increases; on the other hand, the same expressions predict, independently of the value of the spin s , an enhancement of the value of the greybody factor as the number of extra dimensions, that are projected on the brane, increases.

Let us note at this point that the *full analytic* expression Eq. (84) has been derived in the low-energy approximation: the low-energy limit was taken in the expression of the β coefficient, during the matching of the two asymptotic solutions. The *simplified analytic* expressions, Eqs. (88)-(90), have been derived in the same low-energy limit by further expanding Eq. (84). However, it is clear that the more we expand an expression, the more we limit its validity, as more and more terms are left out. The simplified expressions (88)-(90), therefore, are valid in a more narrow low-energy regime than the full analytic one (84). Moreover, the information that we obtain from the simplified expressions is trustable only as long as it is deduced from the lowest partial wave, $j = |s|$, which always gives the main contribution to

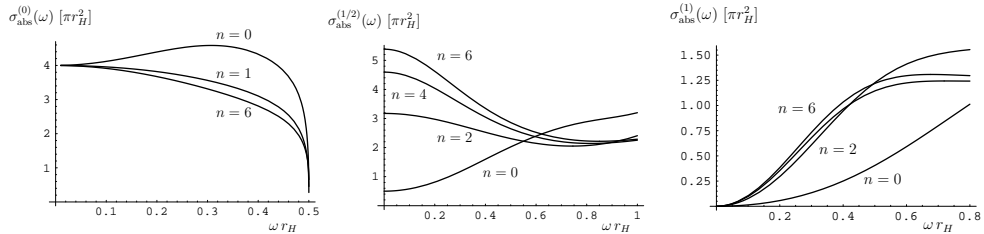


Fig. 1. Analytical results for the greybody factors for emission of (a) scalars, (b) fermions, and (c) gauge bosons from a $(4 + n)$ -dimensional black hole on the brane.

the greybody factor. The aforementioned dependence of $\sigma_{j,n}^{(s)}(\omega)$ on j for all types of fields, as well as the dependence on n for fermions and gauge bosons were indeed derived by looking at the leading term of the lowest partial wave. However, in the case of scalar fields the dominant partial wave ($j = 0$) is found to be independent of n having the form $\sigma_{0,n}^{(0)}(\omega) \simeq 4\pi r_H^2 = A_H$, which is a well-known property of the low-energy behaviour of the greybody factor for scalar fields. One then is forced to look at higher-order terms for the desired dependence on n . Because the higher partial waves are enhanced with n , one may naively conclude that the greybody factor itself increases. However, it turns out that the next-to-leading order terms in the expansion of the lowest partial-wave, denoted by ellipses in Eq. (88), are of the same order as the leading terms of the higher partial waves, and thus should also be taken into account. When this is done, we are finally led to a decrease of the greybody factor for scalar fields with n . An extreme caution is therefore necessary when one deals with simplified expressions as the Eqs. (88)-(90).

On the other hand, for more accurate, and thus more informative, evaluations of the greybody factors and associated emission rates, we clearly need to use the full analytic result (84). Although an approximate result itself, this expression leads to a behaviour for the greybody factors that is in excellent agreement with the exact behaviour in the low-energy regime, and in fairly good agreement with the one in the intermediate-energy regime. Plotting Eq. (84) as a function of the energy parameter ωr_H , for different values of s , leads to the behaviour depicted in Figures 1(a,b,c)¹⁴⁸, where $\sigma_{\text{abs}}^{(s)}$ is the greybody factor (84) summed over j up to the third partial wave – it is easy to see that any higher partial wave has a negligible contribution to the final result in this energy regime. As mentioned above, the greybody factor for scalar fields is found¹⁴⁸ to decrease with n , while the ones for fermions and gauge bosons are enhanced as n increases, at least up to intermediate energies. While scalars and fermions have a non-vanishing greybody factor as $\omega r_H \rightarrow 0$, the one for the gauge bosons vanishes.

The full analytic result for the greybody factor (84) may then be substituted in the expression of the power flux for emission in the four-dimensional spacetime,

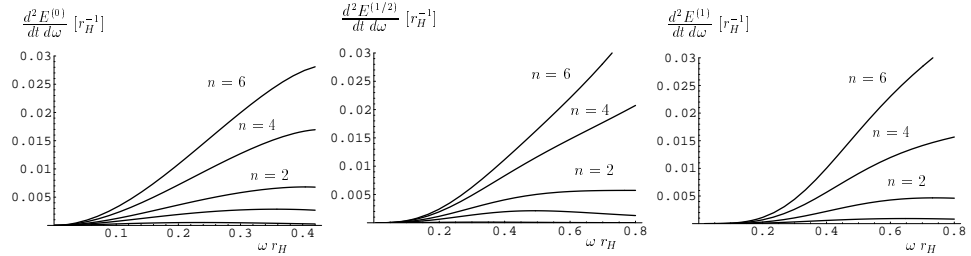


Fig. 2. Analytical results for the energy emission rates for (a) scalars, (b) fermions, and (c) gauge bosons from a $(4+n)$ -dimensional black hole on the brane.

namely

$$\frac{dE^{(s)}(\omega)}{dt} = \sum_j \sigma_{j,n}^{(s)}(\omega) \frac{\omega^3}{\exp(\omega/T_H) \pm 1} \frac{d\omega}{2\pi^2}. \quad (91)$$

Figures 2(a,b,c) depict the behaviour of the energy emission rates for particles with spin 0, $\frac{1}{2}$ and 1 in the low- and intermediate-energy regime. Despite the different low-energy behaviour of the greybody factors for scalars, fermions and gauge bosons, depicted in Figure 1, the corresponding power emission rates, as well as the flux emission rates, exhibit a universal behaviour according to which the energy, and the number of particles, emitted per unit time and energy interval is strongly enhanced, as n increases. This was to be anticipated: we remind the reader that the temperature of the black hole is given by the relation $T_H = (n+1)/4\pi r_H$, therefore, for fixed r_H , the temperature of the black hole increases as n increases. This simply means that the energy of the black hole available for the emission of particles also increases, and this is reflected in the enhancement of the power and flux rates. The effect of the greybody factor, on the other hand, is to suppress or enhance – depending on the spin of the particle, the dimensionality of spacetime and the energy regime that we are looking at – the emission rates compared to the ones derived by using its high-energy, geometrical optics value. This suppression or enhancement is then reflected at the location of the peak of the emission curve. For example, having seen that the greybody factor for gauge bosons is very much suppressed at the low-energy regime, compared to scalars and fermions, we expect that more spin-1 particles will be emitted in the intermediate and high-energy regime, thus shifting the peak of the bosonic emission curve towards higher energies. This feature will indeed be obvious when the complete spectra are derived.

Each one of the curves depicted in Figure 2 has a blackbody profile. Nevertheless, the approximate analytic expression (84) for the greybody factor, and thus the corresponding emission rates, are accurate only in the low-energy regime while at intermediate energies it mainly provides qualitative agreement with the exact behaviour. Any attempt to derive emission rates in the high energy regime by using

this expression is bound to lead to wrong results. For this reason, the graphs in Figure 2 extend only up to intermediate energies for fermions and gauge bosons, while for scalars, our analytic formula breaks down much earlier [see Fig. 1(a)].

Since the analytic results can accurately describe only the part of the “greybody” curve that extends over the low-energy regime, a numerical analysis is clearly necessary in order to derive the complete radiation spectrum. In that case, the master radial equation (53) can be solved through numerical integration¹⁴⁹ under the same boundary conditions that were used in the analytic approach: a purely incoming mode at the horizon of the black hole is integrated outwards until the asymptotic solution (69) is reached. The determination of the asymptotic coefficients, A_- and $A_{in}^{(\infty)}$, can then be used in conjunction with Eq. (79) to define the absorption coefficient, and from that the greybody factors and emission rates¹⁴⁹, as described above. The numerical manipulation of this problem is not without technical difficulties itself: as the spin of the particle increases, it becomes more and more difficult to accurately determine the two asymptotic coefficients; employing various transformations of the radial equation can help remedy this problem (for more information on this point, the reader is referred to Ref. 149).

The numerical integration was performed in Ref. 149 where both greybody factors and emission rates for particles with spin 0, $\frac{1}{2}$ and 1 were computed. The exact results for the greybody factors are displayed in Figures 3(a,b,c). Their complex

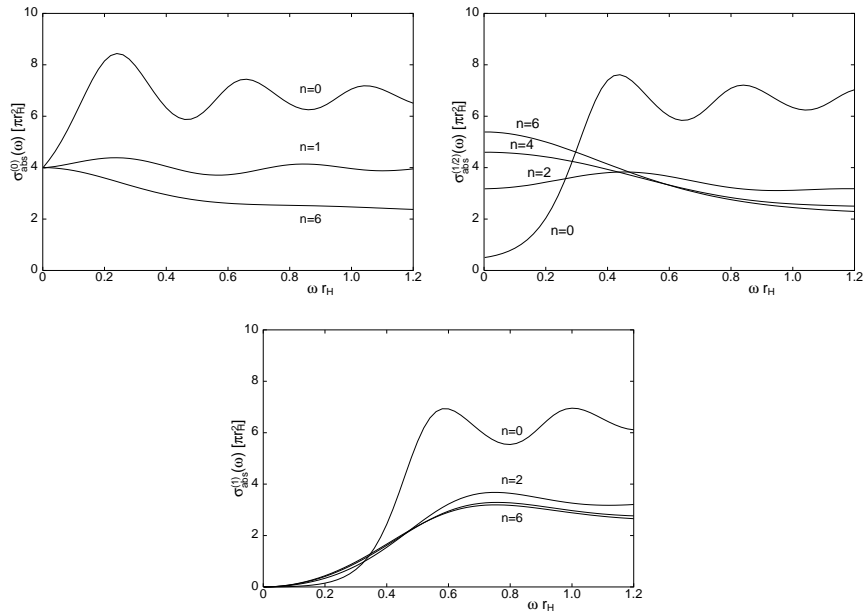


Fig. 3. Numerical results for the greybody factors for emission of (a) scalars, (b) fermions, and (c) gauge bosons from a $(4 + n)$ -dimensional black hole on the brane.

behaviour depending on the spin of the particle emitted, the number of the extra dimensions projected on the brane and the energy regime studied, is evident. At the low-energy regime, the exact results closely follow the ones derived by the analytic method. As $\omega r_H \rightarrow 0$, the greybody factor for scalar fields reduces to $4\pi r_H^2$, thus revealing the fact that the low-energy value of this quantity is indeed proportional to the area of the black hole horizon, even when a number of extra dimensions is projected onto our four-dimensional spacetime. The greybody factor for fermions also reduces to a constant value, different for different values of n , while the one for gauge bosons goes to zero as predicted by the analytic results.

As the energy increases further, the exact results start deviating from the analytic ones and they can be seen adopting an oscillatory behaviour – due to the late dominance of higher partial waves – around a high-energy asymptotic value. This asymptotic value is the same for all particle species, nevertheless it strongly depends on the number of extra dimensions. In this regime, the greybody factor assumes its geometrical optics limit value, already well-known from the four-dimensional case^{118,120,122,123}. For a massless particle in a circular orbit around a black hole, described by the line-element (7), its equation of motion, $p^\mu p_\mu = 0$, takes the form

$$\left(\frac{1}{r} \frac{dr}{d\varphi} \right)^2 = \frac{1}{b^2} - \frac{h(r)}{r^2}, \quad (92)$$

where b is the ratio of the angular momentum of the particle over its linear momentum. The classically accessible regime is defined by the relation $b < \min(r/\sqrt{h})$. Although, the number of the projected dimensions do not change the general structure of the above equation, valid for motion in a four-dimensional, spherically-symmetric background, the expression of the metric function $h(r)$ does change as it carries an explicit dependence on n . Using the definition (55), we can easily find that the closest the particle can get to the black hole is at a distance¹⁵⁴

$$b = r_c \equiv \left(\frac{n+3}{2} \right)^{1/n+1} \sqrt{\frac{n+3}{n+1}} r_H. \quad (93)$$

The above expression correctly reproduces, for $n = 0$, the four-dimensional value of $r_c = 3\sqrt{3}r_H/2$ ^{120,122}. The radius r_c defines the absorptive area of the black hole at high energies and, thus, the corresponding value of the greybody factor, $\sigma_g = \pi r_c^2$, which, being a constant, now describes a blackbody. Since r_c decreases as n increases, the asymptotic greybody factor becomes more and more suppressed as the number of extra dimensions projected onto the brane gets larger.

Turning to the emission rates, the exact results for the energy emission in the form of scalars, fermions and gauge bosons are depicted in Figures 4(a,b,c)¹⁴⁹. The complete emission curves have now been constructed and can be easily compared for different values of n and for different species. For all types of particles, an important enhancement of the energy emission rate takes place, as n increases. This was already predicted by the analytic results, however, the exact numerical results, that are now available, allow us to accurately calculate the enhancement of the emission rates.

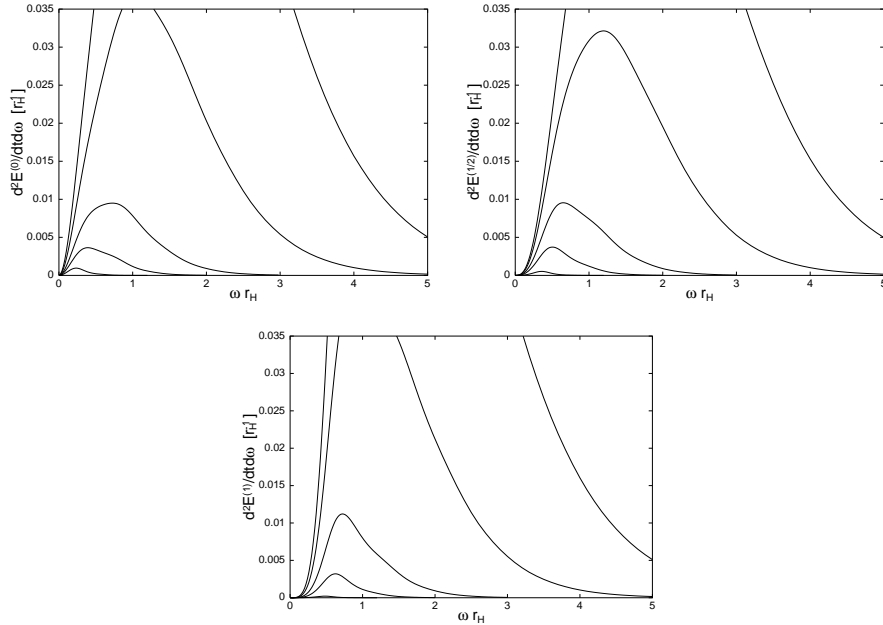


Fig. 4. Numerical results for the energy emission rates for (a) scalars, (b) fermions, and (c) gauge bosons from a $(4 + n)$ -dimensional black hole on the brane.

Integrating over the whole energy regime, we obtain the total energy emissivities, which are displayed in Table 4¹⁴⁹ normalized to the corresponding emissivities for $n = 0$. It is worth pointing out that the amount of energy emitted by the black hole in the case of $n = 7$ is 3 orders of magnitude larger than the one for $n = 0$, for all types of particles. A similar enhancement is observed in the number of particles emitted by the black hole.

Table 4. Total energy emissivities for different values of n

n	0	1	2	3	4	5	6	7
Scalars	1.0	8.94	36.0	99.8	222	429	749	1220
Fermions	1.0	14.2	59.5	162	352	664	1140	1830
Gauge Bosons	1.0	27.1	144	441	1020	2000	3530	5740

Another important question, that one can pose, is what type of particles the black hole ‘prefers’ to emit, as the number of extra dimensions n changes. From the four-dimensional analyses^{118,123} we know that, for $n = 0$, most of the energy of the black hole is emitted in the form of scalar particles; this becomes clear by comparing the areas under the emission curves, for particles with spin 0, $\frac{1}{2}$ and 1, in Figure 5(a). The emission curves in Figure 5(b) have been drawn for $n = 2$: the emission

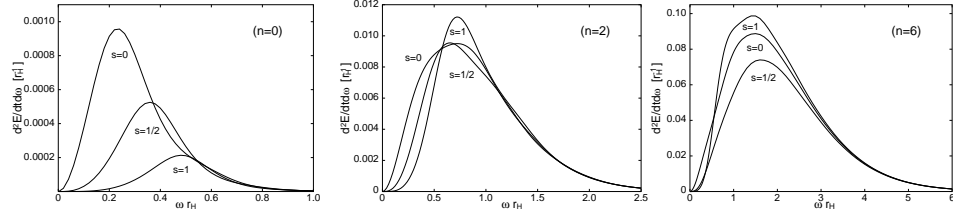


Fig. 5. Energy emission rates for scalars, fermions and gauge bosons for (a) $n = 0$, (b) $n = 2$, and (c) $n = 6$.

curves for scalars, fermions and gauge bosons now seem to define comparable areas. Increasing further the value of n , i.e. $n = 6$, we obtain the emission curves shown in Figure 5(c). The situation has radically changed: the gauge bosons are now the dominant ‘channel’ for the emission of the black hole energy, with the scalars and fermions coming second and third, respectively. Accurate estimates for the relative emissivities have been made¹⁴⁹, and are displayed in Table 5, normalized to the emissivity of scalar fields. The 3-species ratios shown below can equally well be used as signatures for the dimensionality of spacetime if the emitted spectrum of Hawking radiation is successfully observed.

Table 5. Relative energy emissivities for different values of n

n	0	1	2	3	4	5	6	7
Scalars	1.00	1.00	1.00	1.00	1.00	1.00	1.00	1.00
Fermions	0.55	0.87	0.91	0.89	0.87	0.85	0.84	0.82
Gauge Bosons	0.23	0.69	0.91	1.00	1.04	1.06	1.06	1.07

6. Hawking Radiation in the Bulk

We now turn to the study of the Hawking radiation emitted by a small, higher-dimensional black hole in the bulk. According to the assumptions of the model, only gravitons and scalar fields can propagate in the space transverse to the brane, therefore, these are the only modes than should be considered here. Although this type of emission is unlikely to be observed, the study of the bulk emission is extremely important since it determines the amount of energy lost in the bulk, and subsequently the amount of energy left for emission in the form of brane-localized, observable modes.

Due to the simplicity of the metric, the emission of modes from a spherically-symmetric, higher-dimensional black hole was studied first¹⁴⁷. In addition, the absence of any technical difficulties in the derivation of the equation of motion for scalar fields propagating in a higher-dimensional spacetime naturally led to the

study of this particular type of modes first. The emission of bulk scalar modes by a Schwarzschild-like black hole has been studied both analytically^{147,152} and numerically¹⁴⁹. We start by reviewing these results before presenting the definite answer to the question of bulk-to-brane relative emissivity raised above, and before commenting further on the emission of scalar and graviton modes in the bulk.

The gravitational background around a $(4 + n)$ -dimensional, spherically-symmetric black hole is described by the line-element (7)¹¹², which we give again here for convenience

$$ds^2 = -h(r) dt^2 + h(r)^{-1} dr^2 + r^2 d\Omega_{2+n}^2. \quad (94)$$

The equation of motion of a scalar field propagating in the above background is simply given by $D_M D^M \phi = 0$, where D_M is the covariant derivative in the higher-dimensional spacetime. This equation takes a separable form if we use the ansatz

$$\phi(t, r, \theta_i, \varphi) = e^{-i\omega t} R_{\omega\ell}(r) \tilde{Y}_\ell(\Omega), \quad (95)$$

where $\tilde{Y}_\ell(\Omega)$ is the $(3 + n)$ -spatial-dimensional generalization of the usual spherical harmonic functions depending on the angular coordinates¹¹⁵. The radial equation then takes the form¹⁴⁷

$$\frac{h(r)}{r^{n+2}} \frac{d}{dr} \left[h(r) r^{n+2} \frac{dR}{dr} \right] + \left[\omega^2 - \frac{h(r)}{r^2} \ell(\ell + n + 1) \right] R = 0. \quad (96)$$

As in the case of emission on the brane, the above equation must be solved and the absorption coefficient must be determined before we are able to write down the expression for the greybody factor and the emission rates. The same analytic method was also used in this case¹⁴⁷. Eq. (96) was solved in the near-horizon and far-field regime and the two solutions were matched in an intermediate zone. In the near-horizon regime, the same change of variable, $r \rightarrow h(r)$, brings the radial equation to the form

$$h(1-h) \frac{d^2R}{dh^2} + (1-h) \frac{dR}{dh} + \left[\frac{(\omega r_H)^2}{(n+1)^2 h(1-h)} - \frac{\ell(\ell+1+n)}{(n+1)^2(1-h)} \right] R = 0, \quad (97)$$

while the redefinition $R(h) = h^\alpha(1-h)^\beta F(h)$ reduces it to a hypergeometric equation with $a = b = \alpha + \beta$ and $c = 1 + 2\alpha$, where

$$\alpha_\pm = \pm \frac{i\omega r_H}{n+1}, \quad \beta_\pm = \frac{1}{2} \pm \frac{1}{n+1} \sqrt{\left(l + \frac{n+1}{2}\right)^2 - (\omega r_H)^2}. \quad (98)$$

Then, the general solution of Eq. (97) is written as¹⁵¹

$$R_{NH}(h) = A_- h^{\alpha\pm} (1-h)^\beta F(a, b, c; h) + A_+ h^{-\alpha\pm} (1-h)^\beta F(a - c + 1, b - c + 1, 2 - c; h). \quad (99)$$

If we expand the above solution in the limit $r \rightarrow r_H$, or $h \rightarrow 0$, and choose $\alpha = \alpha_-$, we obtain the approximate form

$$R_{NH} \simeq A_- \exp(-i\omega r_H^{n+2} y) + A_+ \exp(i\omega r_H^{n+2} y), \quad (100)$$

in terms of the tortoise coordinate (16). Had we chosen the alternative option $\alpha = \alpha_+$, the same form would have been derived with the coefficients A_- and A_+ interchanged. Since the two options are completely equivalent, we choose the former one, and we demand $A_+ = 0$ in order to have a purely incoming mode near the horizon of the black hole. The criterion of the convergence of the hypergeometric function $\mathbf{Re}(c - a - b) > 0$ demands once again that $\beta = \beta_-$.

In the far-field zone, the limit $r \gg r_H$ and the redefinition $R(r) = f(r)/r^{(n+1)/2}$ reduce Eq. (96) to a Bessel differential equation of the form¹⁴⁷

$$\frac{d^2 f}{dr^2} + \frac{1}{r} \frac{df}{dr} + \left[\omega^2 - \frac{1}{r^2} \left(\ell + \frac{n+1}{2} \right)^2 \right] f = 0. \quad (101)$$

The general solution then for the radial function $R(r)$ is given by¹⁵¹

$$R_{FF}(r) = \frac{B_+}{r^{(n+1)/2}} J_{\ell+(n+1)/2}(\omega r) + \frac{B_-}{r^{(n+1)/2}} Y_{\ell+(n+1)/2}(\omega r), \quad (102)$$

where J and Y are the Bessel functions of the first and second kind, respectively.

In order to match the two asymptotic solutions, the far-field one is expanded in the limit $\omega r \ll 1$, giving

$$R_{FF}(r) \simeq \frac{B_+ r^\ell}{\Gamma(\ell + \frac{n+3}{2})} \left(\frac{\omega}{2} \right)^{\ell+(n+1)/2} - \frac{B_-}{r^{\ell+n+1}} \left(\frac{2}{\omega} \right)^{\ell+(n+1)/2} \frac{\Gamma(\ell + \frac{n+1}{2})}{\pi}, \quad (103)$$

while the near-horizon solution, after being “shifted” and its argument changed to $1 - h$ ¹⁵¹, is expanded in the limit $r \gg r_H$ thus assuming the form

$$R_{NH}(h) \simeq A_- \Gamma(1 + 2\alpha) \left[\left(\frac{r}{r_H} \right)^\ell \frac{\Gamma(1 - 2\beta)}{\Gamma(1 + \alpha - \beta)^2} + \left(\frac{r_H}{r} \right)^{\ell+n+1} \frac{\Gamma(2\beta - 1)}{\Gamma(\alpha + \beta)^2} \right]. \quad (104)$$

Matching the two solutions (103) and (104), we obtain a relation between the two integration constants at infinity

$$\frac{B_+}{B_-} = - \left(\frac{2}{\omega r_H} \right)^{2\ell+n+1} \frac{\Gamma(\ell + \frac{n+1}{2})^2 \left(\ell + \frac{n+1}{2} \right) \Gamma(1 - 2\beta) \Gamma(\alpha + \beta)^2}{\pi \Gamma(1 + \alpha - \beta)^2 \Gamma(2\beta - 1)}. \quad (105)$$

After having completed the determination of the solution for the radial function $R(r)$, we turn our attention to the form of the scalar field at infinity. We need to determine the amplitudes of the incoming and outgoing modes, thus, we expand Eq. (102) in the limit $r \rightarrow \infty$, and we find:

$$R^{(\infty)} = A_{in}^{(\infty)} \frac{e^{-i\omega r}}{\sqrt{r^{n+2}}} + A_{out}^{(\infty)} \frac{e^{i\omega r}}{\sqrt{r^{n+2}}}, \quad (106)$$

with

$$A_{in}^{(\infty)} = \frac{B_+ + iB_-}{\sqrt{2\omega\pi}} e^{i\pi(\ell + \frac{n}{2} + 1)/2}, \quad (107)$$

$$A_{out}^{(\infty)} = \frac{B_+ - iB_-}{\sqrt{2\omega\pi}} e^{-i\pi(\ell + \frac{n}{2} + 1)/2}. \quad (108)$$

The reflection coefficient \mathcal{R}_ℓ is defined as the ratio of the outgoing amplitude over the incoming one at infinity. Then, the absorption coefficient \mathcal{A}_ℓ is given by

$$|\mathcal{A}_\ell|^2 = 1 - |\mathcal{R}_\ell|^2 = 1 - \left| \frac{B_+ - iB_-}{B_+ + iB_-} \right|^2 = \frac{2i(B^* - B)}{BB^* + i(B^* - B) + 1}, \quad (109)$$

where $B \equiv B_+/B_-$ is defined in Eq. (105).

The above analytic result can take a simplified form in the low-energy limit $\omega r_H \ll 1$, in which case $BB^* \gg i(B^* - B) \gg 1$, and we may write

$$|\mathcal{A}_\ell|^2 = \frac{4\pi^2}{2^{4\ell/(n+1)}} \left(\frac{\omega r_H}{2} \right)^{2\ell+n+2} \frac{\Gamma\left(1 + \frac{\ell}{n+1}\right)^2}{\Gamma\left(\frac{1}{2} + \frac{\ell}{n+1}\right)^2 \Gamma\left(\ell + \frac{n+3}{2}\right)^2} + \dots \quad (110)$$

Substituting the above result into Eq. (18), we arrive at¹⁴⁷

$$\sigma_{\ell,n}(\omega) = \frac{\pi}{2^{4\ell/(n+1)}} \left(\frac{\omega r_H}{2} \right)^{2\ell} \frac{\Gamma\left(1 + \frac{\ell}{n+1}\right)^2 \Gamma\left(\frac{n+3}{2}\right)^2}{\Gamma\left(\frac{1}{2} + \frac{\ell}{n+1}\right)^2 \Gamma\left(\ell + \frac{n+3}{2}\right)^2} N_\ell A_H + \dots, \quad (111)$$

where N_ℓ is the multiplicity of states with the same angular momentum number ℓ defined in Eq. (19). Since $\omega r_H \ll 1$, the greybody factor decreases as ℓ increases, therefore, the main contribution to $\sum_\ell \sigma_{\ell,n}$ comes from the lowest partial wave with $\ell = 0$. It is easy to see that the above expression evaluated for $\ell = 0$ simply reduces to A_H , thus, revealing the fact that even in the higher-dimensional case, the greybody factor for scalar fields at the low-energy regime is given by the area of the horizon^f. This behaviour is similar to the one obtained in the four-dimensional case; here, however, the area of the horizon changes as n varies.

As in the four-dimensional case, the contribution to the greybody factor from the dominant partial wave comes out to be independent of the number of extra dimensions. Looking at the dependence of the higher partial waves on n , we obtain a suppression of the greybody factor as the dimensionality of the bulk increases. However, in order to be absolutely certain about this behaviour we would have to include next-to-leading-order corrections in the simplified expression of $\sigma_{\ell,n}(\omega)$ (111), or simply deal with the full analytic result derived from Eq. (109). In either case, however, the derived dependence would only hold in the low-energy regime and no information could be derived from these expressions for the dependence of the greybody factor, and thus of the emission rates, in the high-energy regime.

For this reason, we turn to the numerical integration of the radial equation (96) that can provide exact results for the greybody factor and energy emission rate in the bulk valid at all energy regimes. The behaviour of both these quantities are shown in Figures 6(a,b)¹⁴⁹. As it was predicted by the analytic expression, the greybody factors, normalized to the area of the horizon, tend to unity for all values

^fThis has been recently shown¹⁵³ to hold also for massive scalar particles propagating in a higher-dimensional spacetime.

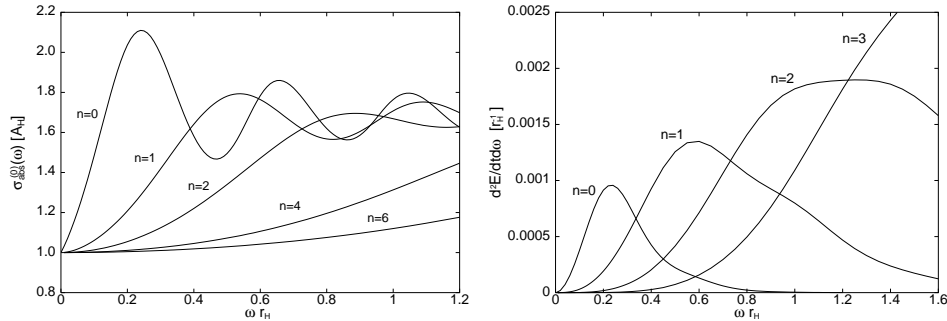


Fig. 6. (a) Greybody factors and (b) energy emission rates for scalar emission in the bulk from a $(4 + n)$ -dimensional black hole.

of n , at the low-energy regime. The naive prediction, also coming from the analytic expression, for the suppression of the greybody factor with n , at the same energy regime, is verified. Similarly to the emission on the brane, as the energy parameter ωr_H increases, the greybody factor oscillates around an asymptotic high-energy limiting value. In analogy with the four-dimensional case, we expect the greybody factor to adopt the $(4 + n)$ -dimensional geometrical optics limit at the high-energy regime. For large values of the energy of the scattered particle, the greybody factor becomes equal to the area of an absorptive body of radius r_c which is projected on a plane parallel to the one of the orbit of the moving particle¹²². We may compute this area by setting one of the azimuthal angles θ_i equal to $\pi/2$ and integrating over the remaining angular coordinates. Then, we find¹⁴⁹

$$A_p = \frac{2\pi}{(n+2)} \frac{\pi^{n/2}}{\Gamma[(n+2)/2]} r_c^{n+2}. \quad (112)$$

The area of the absorptive body is clearly n -dependent, and reduces, as expected, to the usual four-dimensional result $A_p = \pi r_c^2$, for $n = 0$. In the above, r_c is the value of the effective radius defined in Eq. (93)¹⁵⁴. The greybody factor then is given by the above projected area, or more explicitly,

$$\sigma_g = \frac{1}{\sqrt{\pi(n+2)}} \frac{\Gamma[(n+3)/2]}{\Gamma[(n+2)/2]} \left(\frac{n+3}{2}\right)^{(n+2)/(n+1)} \left(\frac{n+3}{n+1}\right)^{(n+2)/2} A_H. \quad (113)$$

In Ref. 149, it was pointed out that the high-energy asymptotic value of the greybody factor, determined through numerical integration, although very close to the ones following from the above analytic expression, did not exactly coincide. However, further study of the asymptotic behaviour revealed that the numerical results do indeed agree with the analytic prediction. The apparent disagreement was due to the fact that the bulk greybody factor adopts its asymptotic value at much higher energies than the brane greybody factor – extending our numerical calculation to higher energies led to the complete agreement with Eq. (113).

According to Figure 6(b), the emission rate of scalar fields in the bulk is enhanced as the number of extra dimensions increases. As with the emission on the brane, this is caused by the increase in the temperature of the black hole, which eventually overcomes the decrease in the value of the greybody factor and causes the enhancement of the emission rate with n at high energies. We can now provide an accurate answer to the question of how much energy is emitted into the bulk compared to the one on the brane. By using Eq. (21), the relative bulk-to-brane energy emission rate may be written as

$$\frac{dE^{(B)}/dt}{dE^{(b)}/dt} = \frac{\sum_\ell N_\ell^{(B)} |\mathcal{A}_\ell^{(B)}|^2}{\sum_\ell N_\ell^{(b)} |\mathcal{A}_\ell^{(b)}|^2}, \quad (114)$$

where the superscripts B and b denote emission in the bulk and brane, respectively. In the above, we have taken into account that bulk and brane modes ‘feel’ the same temperature. The multiplicity of states in the bulk rapidly increases with n , compared to the one on the brane that remains constant. However, it turns out that the enhancement of the absorption probability for brane emission, as n increases, is considerably greater than the one for bulk emission. The exact numerical results derived in Ref. 149 allow us to compute, once again, the total emissivity of the black hole in the bulk and compare it with the one on the brane. The total bulk-to-brane relative emissivities, as a function of n , are given in Table 6¹⁴⁹.

Table 6. Bulk-to-brane energy emissivities for different values of n

n	0	1	2	3	4	5	6	7
Bulk/Brane	1.0	0.40	0.24	0.22	0.24	0.33	0.52	0.93

In Ref. 154, it was shown that the whole tower of KK excitations of a given particle carries approximately the same amount of energy as the massless zero-mode particle emitted on the brane. Combining this result with the fact that many more types of particles live on the brane than in the bulk, it was concluded that most of the energy of the black hole goes into brane modes. The results obtained in Ref. 154 were only approximate since the dependence of the greybody factor on the energy of the emitted particle was ignored and the (low-energy only valid) geometric expression for the area of the horizon was used instead^g. The numerical results reviewed above have used the exact dependence of the greybody factor on both the energy and number of extra dimensions in order to provide the most accurate estimate for the bulk-to-brane energy emissivity. From the entries of the above Table, it becomes clear that the emission of bulk modes for intermediate values of the number of extra dimensions, i.e. $n = 2, 3, 4$ and 5 , is particularly suppressed compared to the one of brane modes. For lower or higher values of n ,

^gIn Ref. 155, it was correctly argued that the dependence of the greybody factor on n must be taken into account, however, the dependence on energy ω was again ignored.

the emission of bulk modes becomes important but the bulk-to-brane ratio never exceeds unity. In conclusion, most of the energy of the higher-dimensional black hole, in the ‘scalar’ channel, is indeed emitted directly on the brane, nevertheless, depending on the number of extra dimensions, a substantial amount of the total energy may be lost in the bulk.

However, a definite conclusion regarding the *total* amount of energy which is lost in the bulk cannot be drawn before the emission of gravitational radiation is also studied. A master equation describing scalar, vector and tensor gravitational perturbations, in a higher-dimensional spherically-symmetric spacetime, was recently derived¹⁵⁶ and was shown to take the form of a 2nd order differential wave equation. At the moment, the interest has been focused on the calculation^{157,158,159,65} of the corresponding quasinormal modes¹⁶⁰, resonances at complex frequencies that dominate at late times after the perturbation of the black hole background (see also^{161,162,163,164,165} for the study of quasinormal modes of scalar fields in the higher-dimensional spacetime). No study addressing the question of the relative bulk-to-brane emission rate for gravitons has yet been done.

The emission of Hawking radiation in the bulk during the spin-down phase has again not been studied as much as the one during the Schwarzschild phase. The equation of motion of a scalar field in a five-dimensional Kerr-like background was shown¹⁶⁶ to take a separable form (just like the Hamilton-Jacobi equations for particles and light propagating in the same background¹⁶⁷) and analytic formulae for the energy and angular momentum fluxes, valid at the low-energy regime, were written down; no quantitative results, however, for the radiation spectra were produced and no generalization of this analysis for arbitrary number of extra dimensions has been carried out. The study of the stability of higher-dimensional, rotating black holes has also attracted some attention: in Ref. 168 it was argued that ‘ultra-spinning’ $(4 + n)$ -dimensional black holes, i.e. with an arbitrarily large angular momentum, are unstable – an earlier work had suggested that black holes with an angular momentum beyond a critical value will ‘decay’ to a rotating black ring¹⁶⁹. On the other hand, perturbations on a massless scalar field propagating in a Kerr-like, higher-dimensional black hole was shown¹⁷⁰ to be free of unstable modes, no matter how large the angular parameter a is. Finally, the stability of a five-dimensional rotating black hole projected onto the brane was checked¹⁷¹, by studying scalar, electromagnetic and gravitational perturbations, and no unstable modes were found in the spectra. It is worth mentioning at this point that the Schwarzschild-like higher-dimensional black holes were shown¹⁷² to be stable under vector and tensor gravitational perturbations, with a potential instability arising only from the scalar gravitational sector, for $n > 2$.

7. Conclusions

The proposal of the existence of extra dimensions in the Universe has opened many different pathways that, in principle, lead to important modifications in the four-

dimensional cosmology, particle physics phenomenology and black hole physics. The recent revival of the idea of the existence of extra space-like dimensions, that can have an almost macroscopic size or be even non-compact, introduced a novel feature in the theory: the scale at which the gravity becomes strong may be much lower than the traditional four-dimensional Planck mass M_P . This has led to the exciting prospect that high-energy collisions between elementary particles, that will take place at next-generation ground-based accelerators or have been already taken place at the atmosphere of the Earth, can probe the energy regime of quantum gravity. Some of the most striking consequences would be the possible creation of mini black holes, or even strings and D-branes, as the products of a high-energy collision of particles with center-of-mass energies at just a few times the new scale of gravity M_* .

In Section 2, we have reviewed the existing results in the literature regarding the possibility of the creation of mini black holes during high-energy collisions. Well-known, four-dimensional analyses have been generalized to cover the case where the colliding particles propagate in a higher-dimensional spacetime. Some of the new studies have shown that, in the case of head-on collisions, the mass of the produced black hole gets suppressed, as the number of extra dimensions increases, while some recent complimentary results indicate that the emission of gravitational waves during the collision is actually suppressed when n increases: this obviously brings the two types of results in an apparent disagreement unless we accept the possibility that a significant amount of the energy, lost during the head-on collision, is emitted in a form different from that of gravitational radiation. On the other hand, for collisions with a non-vanishing impact parameter, which are the most likely to take place, the black hole production cross-section is in fact enhanced with the number of extra dimensions. Putting the above into the framework of a realistic collision between composite particles have led to large estimates, by new physics standards, for the corresponding black hole production cross section, either at the LHC or at the atmosphere of the Earth.

The effect of extra dimensions is not restricted to the production of mini black holes; the properties of the produced, higher-dimensional black holes are also modified. In Section 3, we have discussed some of those properties, namely, the horizon radius, temperature and lifetime, all of which are crucial parameters for the successful production and detection of these elusive, up to now, objects. As we saw, the horizon radius of a $(4 + n)$ -dimensional black hole is many orders of magnitude larger than the one of a four-dimensional black hole with the same mass, which simply means that a mass M needs to be compacted less in a higher-dimensional spacetime to create a black hole. The temperature of these small black holes, in turn, comes out to be lower than in four-dimensions, which means that the emission rate of Hawking radiation is smaller and their lifetime longer. What is most favourable for the possibility of detecting these objects is the fact that, for a black hole with a mass $M_{BH} = 5$ TeV or so, the Hawking radiation spectrum reaches its peak at energies close to the temperature of the black hole which is of the order

of 100-600 GeV (for $n = 1, \dots, 7$); this is exactly the energy regime that present and next-generation collider experiments can probe. Such a small black hole will be extremely short-lived, i.e. $\tau \simeq 10^{-26}$ sec, nevertheless, the proximity of the evaporating black holes to our detectors increases significantly the possibility of their detection.

These mini black holes, upon implementation of quantum effects, emit Hawking radiation into the higher-dimensional spacetime in the form of both bulk and brane modes. The generalization of the four-dimensional expressions for the emission rates in the case of a higher-dimensional spacetime is straightforward, nevertheless, the exact expression of the greybody factors for different types of fields propagating in a higher-dimensional background was, until recently, unknown. As we explained in Section 4, the greybody factors encode valuable information for the background around the emitting black hole and depend on the energy of the emitted particle, its spin and the dimensionality of spacetime. This means that the presence of the greybody factor in the radiation spectrum will cause the modification of the low-energy emission rate from the high-energy one, and will lead to different emissivities for particles with different spin. Moreover, both the number and the type of particles emitted will depend on the number of extra dimensions that exist in nature, a feature that may possibly lead to the determination of the dimensionality of spacetime upon detection of Hawking radiation.

Having concluded that the implementation of the greybody factor in the radiation spectrum is imperative in order to derive accurate estimates for the emission spectrum of the black hole, we moved on, in Section 5, to derive a master equation for the propagation of fields with different spin on the black-hole background induced on the four-dimensional brane. By solving this master equation, one can compute the transmission cross-section, in other words the greybody factor, for brane-localized modes emitted by the black hole. This type of emission during the spin-down phase of a black hole has been only partially studied: radiation spectra for fields with different spin s have been computed only for the case of $n = 1$ in the limit of low energy and low angular momentum. On the contrary, the spherically-symmetric Schwarzschild phase has been thoroughly investigated. Both analytical and numerical methods were used, with the former one leading to analytical, but low-energy-only-valid, expressions, and the latter one yielding exact numerical results valid at all energy regimes. We were thus able to compare the radiation spectra for different types of fields and different number of extra dimensions. For all types of particles, the total emissivities are greatly enhanced with the number of extra dimensions, with the enhancement reaching orders of magnitude for large values of n . As the increase in the emission rate depends strongly on the spin, the relative emissivities for particles with different spin are also strongly n -dependent: while scalar fields remain the preferred type of particle emitted by the black hole for low and intermediate values of n , they are outnumbered by the gauge bosons for large values of n , with the fermions being the least effective channel during the emission.

The emission of brane-localized modes is undoubtedly the most phenomenologically interesting effect since it involves Standard Model particles that can be easily detected during experiments. On the other hand, the emission of bulk modes will be only perceived as a missing energy signal by the observer on the brane. Nevertheless, the amount of energy lost in the bulk is crucially important as it determines the remaining available energy for emission on the brane. The details of the emission of bulk scalar modes during the spin-down phase has been studied in an analytic but qualitative way, and no quantitative results are available. For the Schwarzschild phase, as we saw in section 6, the study has been completed. The greybody factor and emission rates have been calculated and the latter were shown to increase again with the dimensionality of spacetime. The extremely important question of the bulk-to-brane energy emissivity has been answered only for the scalar channel and for the Schwarzschild phase: the amount of energy spent by the black hole for the emission of bulk scalar modes is always smaller than the one for brane modes; nevertheless, the amount of energy lost in the bulk must always be taken into account especially for large values of n when the energies spent in the brane and bulk channel become comparable. No results for the bulk-to-brane emissivity for gravitons have been yet derived.

Although the possibility of the production and evaporation of mini black holes at the LHC is an exciting prospect, this will be possible only in the case where the fundamental scale of gravity M_* is indeed very close to 1 TeV. Nevertheless, there is absolutely no guarantee for that, and the only argument in favour of this particular value is the possible resolution of the hierarchy problem. If M_* is larger than 1 TeV, even by one order of magnitude, the probability of the production of black holes at the LHC vanishes (although we might still witness these type of effects in cosmic ray particles). Nevertheless, all the analytical and numerical results presented in this review have M_* as an independent parameter, and are therefore valid for all values of M_* . If this scale is pushed upwards by various constraints, the derived results will still be applicable for the production and evaporation of black holes at the new energy regime $\sqrt{s} \geq M_*$.

We would also like to stress that the results for the radiation spectra reviewed here refer to individual degrees of freedom and not to elementary particles, like electrons or quarks, which contain more than one polarization. For the number of elementary particles produced, and the energy they carry, one has to use a Black Hole Event Generator^{70,173}. This simulates both the production and decay of small black holes at hadronic colliders and provides estimates for the number and spectra of the different types of elementary particles produced.

In this review, we concentrated on theories postulating the existence of Large Extra Dimensions, and we studied the properties of small black holes that live in a spacetime with $D - 1$ flat spacelike dimensions. Our analysis is definitely not valid in highly curved spacetimes, like the ones in five-dimensional warped models³. In that case, attempts to construct a gravitational background that would reduce to a black-hole line-element on the brane while being well defined away from it

have failed; numerical methods have instead found five-dimensional localized black holes that do not necessarily have a black hole line-element projection onto the brane (see Refs. 174-206 for some relevant works). Nevertheless, in the case of very small bulk cosmological constant, the ‘warping’ of the five-dimensional spacetime, parametrised by the inverse AdS radius, λ^{-1} , is small and the extra spacetime can be considered as an almost flat one. Alternatively, if the horizon radius r_H is much smaller than the AdS radius, no matter what the value of λ is, then the black hole cannot perceive the warping of the fifth dimension. In either case, we may model black holes with $r_H \ll \lambda$ arising in a warped spacetime as black holes living in a five-dimensional, flat spacetime. Under this assumption, all the results presented in this review hold equally well also for the ‘warped’ black holes.

As a concluding remark, we would like to stress once again that the detection of signatures of possible black hole production events during high-energy collisions would be a revolutionary development both for particle physics phenomenology and gravitational physics. Any observational signal of this type would automatically prove the existence of extra dimensions and of a fundamental theory of all forces, with a low energy scale, valid in a higher-dimensional spacetime. The detection of Hawking radiation emitted by these small, higher-dimensional black holes is the most direct evidence for the production and evaporation of those objects. The radiation spectrum of a decaying black hole can also reveal the exact dimensionality of spacetime as both the amount and type of the emitted radiation strongly depend on it. What is also exciting is that a black hole can emit all types of particles that exist in nature, independently of their spin, charge, quantum numbers or interaction properties, as long as their rest mass is smaller than the black hole temperature; therefore, long-sought but yet undiscovered particles, like the Higgs fields or supersymmetric particles, might indeed make their appearance in the decay spectrum of a black hole. The launch of the LHC, or of any other future experiment able to probe even higher energy regimes, deserves to be awaited with great expectations indeed.

Acknowledgments

I would like to thank John March-Russell and Chris. M. Harris for constructive and enjoyable collaborations. This work was funded by the U.K. Particle Physics and Astronomy Research Council (Grant Number PPA/A/S/2002/00350).

References

1. N. Arkani-Hamed, S. Dimopoulos and G. Dvali, *Phys. Lett.* **B429**, 263 (1998); *Phys. Rev.* **D59**, 086004 (1999).
2. I. Antoniadis, N. Arkani-Hamed, S. Dimopoulos and G. R. Dvali, *Phys. Lett.* **B436**, 257 (1998).
3. L. Randall and R. Sundrum, *Phys. Rev. Lett.* **83**, 3370 (1999); *Phys. Rev. Lett.* **83**, 4690 (1999).

4. K. Akama, *Lect. Notes Phys.* **176**, 267 (1982).
5. V. A. Rubakov and M. E. Shaposhnikov, *Phys. Lett.* **B125**, 139 (1983); *Phys. Lett.* **B125**, 136 (1983).
6. M. Visser, *Phys. Lett.* **B159**, 22 (1985).
7. I. Antoniadis, *Phys. Lett.* **B246**, 377 (1990).
8. I. Antoniadis, K. Benakli and M. Quiros, *Phys. Lett.* **331**, 313 (1994).
9. J. Lykken, *Phys. Rev.* **D54**, 3693 (1996).
10. P. Abreu *et al.* [DELPHI Collaboration], *Eur. Phys. J.* **C17**, 53 (2000).
11. G. Abbiendi *et al.* [OPAL Collaboration], *Eur. Phys. J.* **C18**, 253 (2000).
12. D. Acosta *et al.* [CDF Collaboration], *Phys. Rev. Lett.* **89**, 281801 (2002).
13. C. D. Hoyle, U. Schmidt, B. R. Heckel, E. G. Adelberger, J. H. Gundlach, D. J. Kapner and H. E. Swanson, *Phys. Rev. Lett.* **86**, 1418 (2001).
14. L. J. Hall and D. R. Smith, *Phys. Rev.* **D60**, 085008 (1999).
15. S. Cullen and M. Perelstein, *Phys. Rev. Lett.* **83**, 268 (1999).
16. V. D. Barger, T. Han, C. Kao and R. J. Zhang, *Phys. Lett.* **B461**, 34 (1999).
17. C. Hanhart, D. Phillips, S. Reddy and M. Savage, *Nucl. Phys.* **B595**, 335 (2001).
18. C. Hanhart, J. A. Pons, D. R. Phillips and S. Reddy, *Phys. Lett.* **B509**, 1 (2001).
19. R. Allahverdi, C. Bird, S. Groot Nibbelink and M. Pospelov, *Phys. Rev.* **D69**, 045004 (2004).
20. S. Hannestad and G. Raffelt, *Phys. Rev. Lett.* **87**, 051301 (2001).
21. S. Hannestad, *Phys. Rev.* **D64**, 023515 (2001).
22. S. Hannestad and G. Raffelt, *Phys. Rev. Lett.* **88**, 071301 (2002); *Phys. Rev.* **D67**, 125008 (2003) [Erratum-*ibid.* **D69**, 029901 (2004)].
23. L. A. Anchordoqui, J. L. Feng, H. Goldberg and A. D. Shapere, *Phys. Rev.* **D68**, 104025 (2003).
24. K. R. Dienes, E. Dudas and T. Gherghetta, *Phys. Lett.* **B436**, 55 (1998); *Nucl. Phys.* **B537**, 47 (1999).
25. I. Antoniadis, K. Benakli and M. Quiros, *Phys. Lett.* **B460**, 176 (1999).
26. N. Arkani-Hamed, S. Dimopoulos and J. March-Russell, *Phys. Rev.* **D63**, 064020 (2001).
27. R. Sundrum, *Phys. Rev.* **D59**, 085009 (1999).
28. G. F. Giudice, R. Rattazzi and J. D. Wells, *Nucl. Phys.* **B544**, 3 (1999).
29. E. A. Mirabelli, M. Perelstein and M. E. Peskin, *Phys. Rev. Lett.* **82**, 2236 (1999).
30. J. L. Hewett, *Phys. Rev. Lett.* **82**, 4765 (1999).
31. T. Han, J. D. Lykken and R. J. Zhang, *Phys. Rev.* **D59**, 105006 (1999).
32. A. Mazumdar, *Phys. Lett.* **B469**, 55 (1999).
33. N. Arkani-Hamed, S. Dimopoulos, N. Kaloper and J. March-Russell, *Nucl. Phys.* **B567**, 189 (2000).
34. P. Kanti and K. A. Olive, *Phys. Rev.* **D60**, 043502 (1999); *Phys. Lett.* **B464**,

192 (1999); hep-ph/9909535.

35. A. M. Green and J. E. Lidsey, *Phys. Rev.* **D61**, 067301 (2000).
36. N. Kaloper and A. R. Liddle, *Phys. Rev.* **D61**, 123513 (2000).
37. S. Cullen, M. Perelstein and M. E. Peskin, *Phys. Rev.* **D62**, 055012 (2000).
38. N. Kaloper, J. March-Russell, G. D. Starkman and M. Trodden, *Phys. Rev. Lett.* **85**, 928 (2000).
39. U. Gunther and A. Zhuk, *Phys. Rev.* **D61**, 124001 (2000).
40. A. Dedes and P. Kanti, hep-ph/0003051.
41. R. N. Mohapatra, A. Perez-Lorenzana and C. A. de Sousa Pires, *Phys. Rev.* **D62**, 105030 (2000).
42. W. F. Kao, *Phys. Rev.* **D62**, 084009 (2000).
43. A. Mazumdar and A. Perez-Lorenzana, *Phys. Lett.* **B508**, 340 (2001).
44. R. Allahverdi, K. Enqvist, A. Mazumdar and A. Perez-Lorenzana, *Nucl. Phys.* **B618**, 277 (2001).
45. T. Matsuda, *Phys. Rev.* **D66**, 107301 (2002).
46. M. Bastero-Gil, V. Di Clemente and S. F. King, *Phys. Rev.* **D67**, 083504 (2003).
47. B. C. Paul, *Phys. Rev.* **D68**, 127501 (2003).
48. N. D. Birrell and P. C. W. Davies, *Quantum Fields In Curved Space* (Cambridge University Press, Cambridge, 1982).
49. K.A. Khan and R. Penrose, *Nature* **229**, 185 (1971).
50. P. Szekeres, *J. Math. Phys.* **13**, 286 (1972).
51. T. Dray and G. 't Hooft, *Nucl. Phys.* **B253**, 173 (1985); *Class. Quant. Grav.* **3**, 825 (1986).
52. U. Yurtsever, *Phys. Rev.* **D38**, 1706 (1988); *Phys. Rev.* **D38**, 1731 (1988).
53. P. D. D'Eath and P. N. Payne, *Phys. Rev.* **D46**, 658 (1992); *Phys. Rev.* **D46**, 675 (1992); *Phys. Rev.* **D46**, 694 (1992).
54. D. J. Gross and P. F. Mende, *Phys. Lett.* **B197**, 129 (1987); *Nucl. Phys.* **B303**, 407 (1988).
55. D. Amati, M. Ciafaloni and G. Veneziano, *Phys. Lett.* **B197**, 81 (1987); *Int. J. Mod. Phys.* **A3**, 1615 (1988); *Phys. Lett.* **B216**, 41 (1989).
56. G. 't Hooft, *Phys. Lett.* **B198**, 61 (1987); *Nucl. Phys.* **B304**, 867 (1988); *Nucl. Phys.* **B335**, 138 (1990).
57. H. Verlinde and E. Verlinde, *Nucl. Phys.* **B371**, 246 (1992).
58. K. S. Thorne, in *Magic without Magic*, ed. J. R. Klauder (San Francisco, 1972).
59. R. Penrose, presented at the Cambridge University Seminar, *unpublished* (1974).
60. S.W. Hawking and G.F.R. Ellis, *The Large Scale Structure of Spacetime* (Cambridge University Press, New York, 1973).
61. V. Cardoso and J. P. S. Lemos, *Phys. Lett.* **B538**, 1 (2002); *Phys. Rev.* **D67**, 084005 (2003).
62. T. Banks and W. Fischler, hep-th/9906038.

63. D. M. Eardley and S. B. Giddings, *Phys. Rev.* **D66**, 044011 (2002).
64. H. Yoshino and Y. Nambu, *Phys. Rev.* **D66**, 065004 (2002); *Phys. Rev.* **D67**, 024009 (2003).
65. E. Berti, M. Cavaglia and L. Gualtieri, hep-th/0309203.
66. E. Kohlprath and G. Veneziano, *JHEP* **0206**, 057 (2002).
67. D. Ida, K. y. Oda and S. C. Park, *Phys. Rev.* **D67**, 064025 (2003).
68. O. I. Vasilenko, hep-th/0305067.
69. S. B. Giddings and S. Thomas, *Phys. Rev.* **D65**, 056010 (2002).
70. S. Dimopoulos and G. Landsberg, *Phys. Rev.* **D87**, 161602 (2001).
71. S. Dimopoulos and R. Emparan, *Phys. Lett.* **B526**, 393 (2002).
72. S. B. Giddings, hep-ph/0110127.
73. G. F. Giudice, R. Rattazzi and J. D. Wells, *Nucl. Phys.* **B630**, 293 (2002).
74. A. Goyal, A. Gupta and N. Mahajan, *Phys. Rev.* **D63**, 043003 (2001).
75. J. L. Feng and A. D. Shapere, *Phys. Rev. Lett.* **88**, 021303 (2002).
76. L. Anchordoqui and H. Goldberg, *Phys. Rev.* **D65**, 047502 (2002).
77. R. Emparan, M. Masip and R. Rattazzi, *Phys. Rev.* **D65**, 064023 (2002).
78. S. Hossenfelder, S. Hofmann, M. Bleicher and H. Stocker, *Phys. Rev.* **D66**, 101502 (2002); *Phys. Lett.* **B548**, 73 (2002).
79. H. C. Kim, S. H. Moon and J. H. Yee, *JHEP* **0202**, 046 (2002).
80. K. Cheung, *Phys. Rev. Lett.* **88**, 221602 (2002); *Phys. Rev.* **D66**, 036007 (2002).
81. R. Casadio and B. Harms, *Int. J. Mod. Phys.* **A17**, 4635 (2002).
82. S. C. Park and H. S. Song, *J. Korean Phys. Soc.* **43**, 30 (2003).
83. G. Landsberg, *Phys. Rev. Lett.* **88**, 181801 (2002); hep-ex/0310034.
84. E. J. Ahn, M. Cavaglia and A. V. Olinto, *Phys. Lett.* **B551**, 1 (2003).
85. Y. Uehara, hep-ph/0205199.
86. R. Guedens, D. Clancy and A. R. Liddle, *Phys. Rev.* **D66**, 043513 (2002).
87. A. V. Kotwal and C. Hays, *Phys. Rev.* **D66**, 116005 (2002).
88. A. Chamblin and G. C. Nayak, *Phys. Rev.* **D66**, 091901 (2002).
89. T. Han, G. D. Kribs and B. McElrath, *Phys. Rev. Lett.* **90**, 031601 (2003).
90. L. Anchordoqui and H. Goldberg, *Phys. Rev.* **D67**, 064010 (2003).
91. M. Cavaglia, *Int. J. Mod. Phys.* **A18**, 1843 (2003).
92. A. Chamblin, F. Cooper and G. C. Nayak, hep-ph/0301239.
93. I. Mocioiu, Y. Nara and I. Sarcevic, *Phys. Lett.* **B557**, 87 (2003).
94. R. Casadio, *Annals Phys.* **307**, 195 (2003).
95. L. A. Anchordoqui, J. L. Feng, H. Goldberg and A. D. Shapere, *Phys. Rev.* **65**, 124027 (2002); hep-ph/0311365.
96. Y. Uehara, *Prog. Theor. Phys.* **107**, 621 (2002).
97. J. Alvarez-Muniz, J. L. Feng, F. Halzen, T. Han and D. Hooper, *Phys. Rev.* **D65**, 124015 (2002).
98. A. Ringwald and H. Tu, *Phys. Lett.* **B525**, 135 (2002).
99. M. Kowalski, A. Ringwald and H. Tu, *Phys. Lett.* **B529**, 1 (2002).

100. D. Kazanas and A. Nicolaidis, *Gen. Rel. Grav.* **35**, 1117 (2003).
101. P. Jain, S. Kar, S. Panda and J. P. Ralston, *Int. J. Mod. Phys. D* **12**, 1593 (2003).
102. A. Ringwald, *Fortsch. Phys.* **51**, 830 (2003).
103. E. J. Ahn, M. Ave, M. Cavaglia and A. V. Olinto, *Phys. Rev. D* **68**, 043004 (2003).
104. A. Nicolaidis and N. G. Sanchez, hep-ph/0307321.
105. A. Barrau, J. Grain and S. O. Alexeyev, hep-ph/0311238.
106. M. B. Voloshin, *Phys. Lett. B* **518**, 137 (2001); *Phys. Lett. B* **524**, 376 (2002).
107. S. N. Solodukhin, *Phys. Lett. B* **533**, 153 (2002).
108. T. G. Rizzo, *JHEP* **0202**, 011 (2002).
109. S. D. H. Hsu, *Phys. Lett. B* **555**, 92 (2003).
110. M. Cavaglia, S. Das and R. Maartens, *Class. Quant. Grav.* **20**, L205 (2003).
111. V. S. Rychkov, hep-ph/0401116.
112. R. C. Myers and M. J. Perry, *Annals Phys.* **172**, 304 (1986).
113. P. C. Argyres, S. Dimopoulos and J. March-Russell, *Phys. Lett. B* **441**, 96 (1998).
114. S. W. Hawking, *Commun. Math. Phys.* **43**, 199 (1975).
115. C. Muller, in *Lecture Notes in Mathematics: Spherical Harmonics* (Springer-Verlag, Berlin-Heidelberg, 1966).
116. S. S. Gubser, I. R. Klebanov and A. A. Tseytlin, *Nucl. Phys. B* **499**, 217 (1997).
117. M. Bander and C. Itzykson, *Rev. Mod. Phys.* **38**, 330 (1966).
118. D. N. Page, *Phys. Rev. D* **13**, 198 (1976).
119. W. G. Unruh, *Phys. Rev. D* **14**, 3251 (1976).
120. N. Sanchez, *Phys. Rev. D* **16**, 937 (1977); *Phys. Rev. D* **18**, 1030 (1978); *Phys. Rev. D* **18**, 1798 (1978).
121. D. N. Page, *Phys. Rev. D* **14**, 3260 (1976).
122. C. W. Misner, K. T. Thorne and J. A. Wheeler, *Gravitation* (Freeman, San Francisco, 1973).
123. J. H. MacGibbon and B. R. Webber, *Phys. Rev. D* **41**, 3052 (1990).
124. W. T. Zaumen, *Nature* **247**, 530 (1974).
125. G. W. Gibbons, *Commun. Math. Phys.* **44**, 245 (1975).
126. B. Carter, *Phys. Rev. Lett.* **33**, 558 (1974).
127. D. N. Page, *Phys. Rev. D* **14**, 1509 (1976); *Phys. Rev. D* **16**, 2402 (1977).
128. E. Newman and R. Penrose, *J. Math. Phys.* **3**, 566 (1962).
129. S. Chandrasekhar, *The Mathematical Theory of Black Holes* (Oxford University Press, New York, 1983).
130. C. Flammer, *Spheroidal Wave Functions* (Stanford University Press, Stanford, USA, 1957).
131. J. N. Goldberg, A. J. MacFarlane, E. T. Newman, F. Rohrlich and E. C. Sudarshan, *J. Math. Phys.* **8**, 2155 (1967).
132. S. A. Teukolsky, *Phys. Rev. Lett.* **29**, 1114 (1972); *Astrophys. J.* **185**, 635

(1973).

133. W. H. Press and S. A. Teukolsky, *Astrophys. J.* **185**, 649 (1973); *Astrophys. J.* **193**, 443 (1974).

134. D. R. Brill, P. L. Chrzanowski, C. Martin Pereira, E. D. Fackerell and J. R. Ipser, *Phys. Rev.* **D5**, 1913 (1972).

135. A. A. Starobinskii and S. M. Churilov, *Sov. Phys.-JETP* **38**, 1 (1974).

136. E. D. Fackerell and R. G. Crossman, *J. Math. Phys.* **18**, 1849 (1977).

137. E. Seidel, *Class. Quant. Grav.* **6**, 1057 (1989).

138. S. R. Das and S. D. Mathur, *Nucl. Phys.* **B478**, 561 (1996).

139. S. R. Das, G. W. Gibbons and S. D. Mathur, *Phys. Rev. Lett.* **78**, 417 (1997).

140. J. M. Maldacena and A. Strominger, *Phys. Rev.* **D55**, 861 (1997).

141. I. R. Klebanov, *Nucl. Phys.* **B496**, 231 (1997).

142. M. Cvetic and F. Larsen, *Nucl. Phys.* **B506**, 107 (1997).

143. S. S. Gubser, *Phys. Rev.* **D56**, 7854 (1997).

144. K. Hosomichi, *Nucl. Phys.* **B524**, 312 (1998).

145. M. Cvetic and F. Larsen, *Phys. Rev.* **D57**, 6297 (1998).

146. H. W. Lee and Y. S. Myung, *Phys. Rev.* **D58**, 104013 (1998).

147. P. Kanti and J. March-Russell, *Phys. Rev.* **D66**, 024023 (2002).

148. P. Kanti and J. March-Russell, *Phys. Rev.* **D67**, 104019 (2003).

149. C. M. Harris and P. Kanti, *JHEP* **0310**, 014 (2003).

150. P. Kanti, hep-ph/0310162.

151. M. Abramowitz and I. Stegun, *Handbook of Mathematical Functions* (Academic, New York, 1996).

152. V. Frolov and D. Stojkovic, *Phys. Rev.* **D66**, 084002 (2002); *Phys. Rev. Lett.* **89**, 151302 (2002).

153. E. I. Jung, S. H. Kim and D. K. Park, hep-th/0311036.

154. R. Emparan, G. T. Horowitz and R. C. Myers, *Phys. Rev. Lett.* **85**, 499 (2000).

155. M. Cavaglia, *Phys. Lett.* **B569**, 7 (2003).

156. H. Kodama and A. Ishibashi, *Prog. Theor. Phys.* **110**, 701 (2003); hep-th/0308128.

157. V. Cardoso, O. J. C. Dias and J. P. S. Lemos, *Phys. Rev.* **D67**, 064026 (2003).

158. R. A. Konoplya, *Phys. Rev.* **D68**, 124017 (2003).

159. V. Cardoso, J. P. S. Lemos and S. Yoshida, *JHEP* **0312**, 041 (2003); gr-qc/0309112.

160. K. D. Kokkotas and B. G. Schmidt, *Living Rev. Rel.* **2**, 2 (1999).

161. G. T. Horowitz and V. E. Hubeny, *Phys. Rev.* **D62**, 024027 (2000).

162. R. A. Konoplya, *Phys. Rev.* **D66**, 044009 (2002); *Phys. Rev.* **D68**, 024018 (2003).

163. C. Molina, *Phys. Rev.* **D68**, 064007 (2003).

164. V. Cardoso, S. Yoshida, O. J. C. Dias and J. P. S. Lemos, *Phys. Rev.* **D68**, 061503 (2003).

165. G. Siopsis, hep-th/0402083.

166. V. Frolov and D. Stojkovic, *Phys. Rev.* **D67**, 084004 (2003).
167. V. Frolov and D. Stojkovic, *Phys. Rev.* **D68**, 064011 (2003).
168. R. Emparan and R. C. Myers, *JHEP* **0309**, 025 (2003).
169. R. Emparan and H. S. Reall, *Phys. Rev. Lett.* **88**, 101101 (2002).
170. D. Ida, Y. Uchida and Y. Morisawa, *Phys. Rev.* **D67**, 084019 (2003).
171. E. Berti, K. D. Kokkotas and E. Papantonopoulos, *Phys. Rev.* **D68**, 064020 (2003).
172. A. Ishibashi and H. Kodama, *Prog. Theor. Phys.* **110**, 901 (2003).
173. C. M. Harris, P. Richardson and B. R. Webber, *JHEP* **0308**, 033 (2003).
174. A. Chamblin, S. W. Hawking and H. S. Reall, *Phys. Rev.* **D61**, 065007 (2000).
175. R. Gregory and R. Laflamme, *Phys. Rev. Lett.* **70**, 2837 (1993).
176. R. Emparan, G. T. Horowitz and R. C. Myers, *JHEP* **0001**, 007 (2000).
177. J. Garriga and M. Sasaki, *Phys. Rev.* **D62**, 043523 (2000).
178. A. Chamblin, C. Csaki, J. Erlich and T. Hollowood, *Phys. Rev.* **D62**, 044012 (2000).
179. N. Dadhich, R. Maartens, P. Papadopoulos and V. Rezania, *Phys. Lett.* **B487**, 1 (2000).
180. S. Nojiri, O. Obregon, S. D. Odintsov and S. Ogushi, *Phys. Rev.* **D62**, 064017 (2000).
181. R. Gregory, *Class. Quant. Grav.* **17**, L125 (2000); *Phys. Lett.* **B547**, 55 (2002); *JHEP* **0306**, 041 (2003).
182. A. Chamblin, H. S. Reall, H. a. Shinkai and T. Shiromizu, *Phys. Rev.* **D63**, 064015 (2001).
183. I. Giannakis and H. c. Ren, *Phys. Rev.* **D63**, 024001 (2001); *Phys. Rev.* **D64**, 065015 (2001); *Phys. Lett.* **B528**, 133 (2002).
184. R. Emparan, R. Gregory and C. Santos, *Phys. Rev.* **D63**, 104022 (2001).
185. C. Charmousis, R. Emparan and R. Gregory, *JHEP* **0105**, 026 (2001).
186. M. S. Modgil, S. Panda and G. Sengupta, *Mod. Phys. Lett.* **A17**, 1479 (2002).
187. M. Bruni, C. Germani and R. Maartens, *Phys. Rev. Lett.* **87**, 231302 (2001).
188. M. Govender and N. Dadhich, *Phys. Lett.* **B538**, 233 (2002).
189. M. Rogatko, *Phys. Rev.* **D64**, 064014 (2001).
190. P. Kanti and K. Tamvakis, *Phys. Rev.* **D65**, 084010 (2002).
191. T. Wiseman, *Phys. Rev.* **D65**, 124007 (2002); *Class. Quant. Grav.* **20**, 1137 (2003).
192. R. Casadio, A. Fabbri and L. Mazzacurati, *Phys. Rev.* **D65**, 084040 (2002).
193. S. I. Vacaru and D. Singleton, *Class. Quant. Grav.* **19**, 3583 (2002).
194. R. Casadio and L. Mazzacurati, *Mod. Phys. Lett.* **A18**, 651 (2003).
195. R. Emparan, A. Fabbri and N. Kaloper, *JHEP* **0208**, 043 (2002).
196. R. Neves and C. Vaz, *Phys. Rev.* **D66**, 124002 (2002); *Phys. Rev.* **D68**, 024007 (2003); *Phys. Lett.* **D568**, 153 (2003).
197. P. Kanti, I. Olasagasti and K. Tamvakis, *Phys. Rev.* **D66**, 104026 (2002); *Phys. Rev.* **D68**, 124001 (2003).

198. G. Kofinas, E. Papantonopoulos and V. Zamarias, *Phys. Rev.* **D66**, 104028 (2002).
199. R. Emparan, J. Garcia-Bellido and N. Kaloper, *JHEP* **0301**, 079 (2003).
200. H. Kudoh, T. Tanaka and T. Nakamura, *Phys. Rev.* **D68**, 024035 (2003).
201. K. A. Bronnikov, V. N. Melnikov and H. Dehnen, *Phys. Rev.* **D68**, 024025 (2003).
202. S. Shankaranarayanan and N. Dadhich, gr-qc/0306111.
203. C. Charmousis and R. Gregory, *Class. Quant. Grav.* **21**, 527 (2004).
204. T. Tamaki, S. Kanno and J. Soda, *Phys. Rev.* **D69**, 024010 (2004).
205. R. Maartens, gr-qc/0312059.
206. H. Kudoh, hep-th/0401229.